

Coherence Function of Wind and Waves of Metocean Data

By

Quailid Rezza Bin Mohamad Nasir

10969

(Supervisor: AP Ir Dr Shahir Liew)

A project dissertation submitted to the

Civil Engineering Programme

Universiti Teknologi PETRONAS

In partial fulfilment of the requirement for the

BACHELOR OF ENGINEERING (HONS)

(CIVIL ENGINEERING)

Universiti Teknologi PETRONAS

Bandar Seri Iskandar

31750 Tronoh

Perak Darul Ridzuan

CERTIFICATION OF APPROVAL

Coherence Function of Wind and Waves of Metocean Data

by

Quailid Rezza Bin Mohamad Nasir

A project dissertation submitted to the

Civil Engineering Programme

Universiti Teknologi PETRONAS

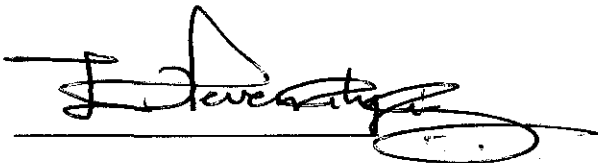
In partial fulfilment of the requirement for the

BACHELOR OF ENGINEERING (Hons)

(CIVIL ENGINEERING)

SEPTEMBER 2011

Approved by,

A handwritten signature in black ink, appearing to read 'M. Shahir Liew', is written over a horizontal line. The signature is stylized and includes a large loop at the end.

(AP Ir. Dr. Mohd Shahir Liew)

CERTIFICATION OF ORIGINALITY

This is to certify that I am responsible for the work submitted in this project, that the original work is my own except as specified in the references and acknowledgement, and the original work contained herein have not been undertaken or done by unspecified sources of persons.



QUAILID REZZA BIN MOHAMAD NASIR

ABSTRACT

In this paper, a research regarding analysis of metocean data is done that includes two main parameters; wind and waves. The objective of this project is mainly to apply Coherence Function as the mechanism tool for frequency domain analysis of a linear system between wind and wave from the full scale metocean data of three platforms located in different operating field. From here we are able to determine the correlation of these environmental forces to estimate the significance frequency where these forces acts in linear functions in the system, thus identify the response of the platform structural members as we assume the inputs to be stationary. It is very crucial to determine the response of the structural members so that we can improve the platform design standards and also as approaches to standard maintenance procedures. This project will focus on the metocean data collected from each platform for different field operation; Dulang-B platform from Peninsular Malaysia Operation (PMO), Tukai platform form Sarawak Operation (SWO) and Samarang platform from Sabah Operation (SBO). This is to ensure that we are able to distinguish the environmental condition for each set of metocean data as well as the seasonal pattern. The measured data is analyzed using the assistance of mathematical software, PASW 18 in order to compute the complex algorithm involved. The results obtained show that the wind is not actually the major factor to generate the wave at specific platforms. It is estimated up to 30% only while other factors that contribute to generate wave are possibly the tidal effect, gravity pull or other parts of the sea. The coherency differs for platform at different operation field region, as well as for seasonal pattern. The highest coherency recorded is the interaction of wind and waves at Tukai during non monsoon season, where the interaction of both forces optimum at frequency 0.1Hz, while other platforms show a true non linear relationship of wind and waves. However during monsoon season shows the other way around where Dulang-B platform and Samarang shows a quite similar seasonal pattern, but slightly differs in the coherency range.

ACKNOWLEDGEMENT

Be praised upon Him, who gives me the strength to put all the effort in order to complete this project and enough time to meet the deadline as scheduled. First of all, I would like to express my gratitude to my supervisor Assoc. Prof. Ir. Dr. Mohd Shahir Liew for giving me a very well assistance and guidance throughout the entire project. The credits also should be given to him for the exposure and opportunity given to me to involve with the experts from industrial sectors.

In addition, I am thankful to all the research team members involved with the PETRONAS Carigali Sdn Bhd. grant project, who works really hard along with me in order to make this project a success. Same goes to all the colleagues, post-graduates student and also peers who deserve the credits that are not mention.

Last but not least, I would like to thanks the Civil Department for giving me the opportunity to excel in this field and all the Civil Engineering students that have contributed to this project either directly or indirectly in making this study a success.

Thank you.

LIST OF FIGURES

1)	Schematic Representation of a Linear System	2
2)	Dulang-B Platform	4
3)	Tukau Platform	4
4)	Samarang Platform	4
5)	Acoustic Doppler Current Profiler (ADCP)	5
6)	Wave parameters	8
7)	Coherence Function value	12
8)	Time Series Analysis	16
9)	Histogram of significant wave height at Gulf of Mexico	17
10)	FYP2 Gantt Chart	19
11)	FYP2 Milestone	20
12)	Coherence Function of Wind and Waves for Dulang B Platform in 2000	21
13)	Coherence Function of Wind and Waves for Samarang Platform in 2000	22
14)	Coherence Function of Wind and Waves for Tukau Platform in 2000	23
15)	Coherence Function of Wind and Waves during Monsoon Season in 2000	24
16)	Coherence Function of Wind and Waves during Non Monsoon in 2000	25

LIST OF TABLES

1)	Metocean data available	3
2)	Selected platforms details	3
3)	Suggested minimum requirements to recording intervals, averaging period and sampling frequency	6
4)	Coherence Function Table of Wind and Waves for Dulang B Platform in 2000	21
5)	Coherence Function Table of Wind and Waves for Samarang Platform in 2000	22
6)	Coherence Function Table of Wind and Waves for Tukai Platform in 2000	23
7)	Coherence Function Table of Wind and Waves during Monsoon Season in 2000	24
8)	Coherence Function of Wind and Waves during Non Monsoon in 2000	25

TABLE OF CONTENT

1.0	INTRODUCTION	
1.1	Background Study	1
1.2	Problem Statement	2
1.3	Objective	2
1.4	Scope of Study	3
2.0	LITERATURE REVIEW	
2.1	Metoccean data and Parameters	5
2.2	Wave Loads	6
2.2.1	Wave Theory	8
2.2.2	Wave Statistics	9
2.2.3	Wave Forces on Structural Members	9
2.3	Wind Loads	10
2.4	Coherence Function	11
2.4.1	Interpretation of Coherence Function	12
2.4.2	Noise reduction by using Coherence Function	13
2.4.3	Multivariate Coherence Function	14
2.4.4	Cross-Spectrum	15
3.0	METHODOLOGY	
3.1	Method Used	16
3.1.1	Amplitude Domain	17
3.1.2	Time Domain	18
3.1.3	Frequency Domain	18
3.2	Software Used	19
3.2.1	Microsoft Excel	19
3.2.2	PASW Statistic Software for computer	19
3.3	Activities	19
3.3.1	Gantt Chart	19
3.3.2	Milestone	20
4.0	RESULTS & DISCUSSION	
4.1	Coherency for Seasonal Pattern	21
4.1.1	Dulang-B Platform (PMO)	21
4.1.2	Samarang Platform (SBO)	22
4.1.3	Tukau Platform (SKO)	23
4.2	Coherency for Different Operation Field	24
4.2.1	Monsoon Season	24
4.2.2	Non Monsoon Season	25
5.0	RECOMMENDATIONS	26
6.0	CONCLUSION	27
7.0	REFERENCES	28
	APPENDICES	29

CHAPTER 1

INTRODUCTION

1.1 Background of Study

Nowadays, with rapid development of technology as well researches in engineering field had improved and created a firm base for oil industrial. As more oil platform is constructed for purpose of exploration, the structure design is vital in order to accomplish the mission along the process. Rather than concerning the basic loads such as dead loads and live loads for the structure design, offshore structure brings in more complexity in terms of force to be dealt. The environmental criteria need to be considered as natural forces such as wind, waves and current is somehow highly significance for the design calculation with mass coefficient and drag coefficient taken into account.

Most of the platform structures in Malaysia currently are design based on *API* and *PTS* which is categorised as traditional, since *PTS* is established for almost 20 years back [6]. In general, two principal are considered during the global design of structures. These are the storm (or extreme event) condition and the operational (or normal) condition. For the design purpose, extreme values associate with return periods of 100 years are estimated to fulfil the requirement. A high level of data accuracy is essential for a proper design of a platform.

Throughout these years, there is numerous time series analysis method is introduced. As a form of data manipulation, it has been richly develop for a wide assortment of application. These data are presented in amplitude domain, time domain and frequency domain. Later there will be two main parts for the result section in order to make a clear view of the findings. The first section is the results of the coherency for seasonal pattern. This section allows us to distinguish the seasonal pattern for a specific platform in a particular year. For the second section, it will be the results of the coherency for different operation field platform. From here we are able to compare the environmental condition of a different operation field.

1.2 Problem Statement

As we all know, wave, wind and current have been affecting the platform structure. These are the forces that are the most challenging factors for the designing stage of offshore structure, instead the basic design of the primary structure. The structure is to be designed to the extreme value of the natural forces and exceeding the limits, so that it will sustain due to the impact since we are not able to forecast or estimate the exact forces that will acting on the structure. However we are able to measure and determine to the highest possibility for the range of fluctuation of the wind and waves base on direct measure that actually can be done for 100 years return period.

The behaviour of every steel members of the structure especially at jacket, are acting due to wave forces, and wind forces. In order to determine the response of the structure members due to these natural forces, we have to study the similarities and the significance of these forces as the input signal into the system that will be analyse in frequency domain.

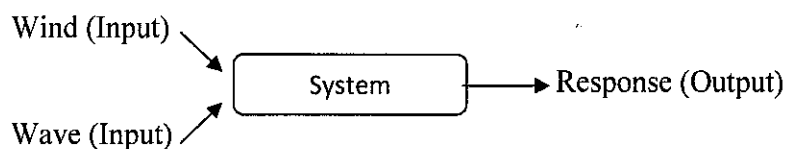


Figure 1: Schematic Representation of a Linear System

1.3 Objective

The main objective is to apply Coherence Function as the mechanism tool for frequency domain analysis of a linear system between wind and wave from the full scale metocean data of three platforms located in different operating field. From here we are able to obtain the dominating factor from the environmental loads as well as the linearity between the interaction of wind and waves. Besides, we are able to distinguish the seasonal pattern of monsoon and non monsoon season for each platform and also the environmental factors of considering different operation field region in a specific season.

1.4 Scope of Study

Basically, this paper will cover the analysis for wind and waves for Dulang B platform, Samarang platform and Tukai platform. The metocean data is collected from Petronas Carigali Sdn. Bhd. (PCSB). The table below shows the raw data available and selected platforms as highlighted:

REGION	FIELD	DATA	PERIOD
PMO	DULANG	wind/ wave	1999-2006
	BEKOK	wind/wave	2001-2009
SKO	TUKAU	wind/ wave	1999-2003
	BARONIA	wind/ wave	1999-2003
	BARONIA	current	2006-2007
SBO	ERB WEST	wind/ wave	1999-2003
	SAMARANG	wind/ wave	1999-2003
	SUMANDAK	current	2002

Table 1: Metocean data available

Below are the details of the respective platform:

Operation Basin	Penisular Malaysia	Sarawak	Sabah
Platform	Dulang B	TKQ-A	SMQ-A
Field	Dulang	Tukai	Samarang
Platform Type	Fixed Steel Jacket	Fixed Steel Jacket	Fixed Steel Jacket
Platform Function	Production/Drilling/ Accommodation	Accommodation	Accommodation
Installed	1990	01/01/1982	01/01/1984
Oil Prod (Avg) ³	12, 428 BOPD	0.0 BOPD	0.0 BOPD
Gas Prod (Avg) ³	0.0 MCFD	0.0 MCFD	0.0 MCFD
Latitude	5° 49' 44.947" N	4° 24' 47.181" N	5° 37' 07.686" N
Longitude	104° 09' 25.900" E	113° 43' 40.767" E	114° 53' 18.959" E
Water Depth	79.2m	46.3m	10.1m

Table 2: Selected platforms details.

CHAPTER 2

LITERATURE REVIEW

2.1 Metocean data and parameter

Meteorological data i.e. wind, atmospheric pressure and air temperature, and oceanographic data i.e. waves, current, water level, salinity and water temperature are often not only lumped together in the term metocean data, but are also typically lumped together in one design basis for environmental parameters. Furthermore, the two sets of parameters are deeply related as the meteorological conditions are the driving forces for waves, surge levels and currents. The term *hydrographic* data is often used for the oceanographic data.

The main sources from where to obtain metocean data vary from the very initial stages of a project to the detailed design stage as the requirement to accuracy and reliability increases. In the initial stages global data from the area or nearby areas may serve as a first set of information. However, caution in use of such data is warranted, in particular if the data source refers to deeper waters than the wind farm site. Global data can be found in summary statistics based on reported and analyzed ship observations, from satellite measurements or from public measurement campaigns.

Metocean data is obtained from in-situ measurement, using high technology tools and equipments such as *Acoustic Doppler Current Profiler (ADCP)*, wave buoy, radar, pressure gauge etc. are commonly used for measuring oceanographic data.

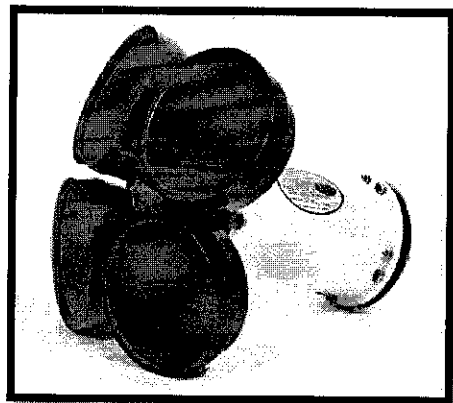


Figure 5: Acoustic Doppler Current Profiler (ADCP) is used for measuring oceanographic data.

Besides that, metocean (meteorological and oceanographic) data is collected and refers to the use of historical meteorological data to drive numerical models for water level, current and waves, which is called *Hindcast* methodology. It is noted that the use of hindcast data implies an assumption of the past being representative for future conditions in a statistical sense. Effects of possible changes in climate should be considered in the final analysis.

Various public documents can assist in defining the requirements to measurement campaign in term of recording intervals, accuracy, resolution and data analysis. Below are the table that summarize suggested minimum values for recording intervals, averaging period and sampling frequency. [1]

Parameter	Recording Interval	Averaging Period	Sampling Frequency
Waves	1 hour	20 min	2.5 Hz
Currents	10 min	10 min	1 Hz
Water Levels	10 min	1 min	1 Hz

Table 3: Suggested minimum requirements to recording intervals, averaging period and sampling frequency. [1]

2.2 Wave Loads

The wave loading of an offshore structure is usually the most important of all environmental loadings for which the structure must be designed. The forces on the structure are caused by the motion of the water due to the waves which are generated by the action of the wind on the surface of the sea. It is also considered as dynamic load and tends to be stochastic in nature. Dynamic loads are any loads for which the magnitude, direction, position, or any combination of these varies with time [8]. Dynamic loads can be characterized as either deterministic or non-deterministic. If the time variation of the loads is fully known, then they are classified as deterministic loads. When the time variation of the loads is not fully known, then they are classified as non-deterministic or stochastic loads. Non-deterministic loads can be treated as random processes because at any point in time, these loadings are random variables.

Determination of these forces requires the solution of two separate, though interrelated problems. The first is the sea state computed using an idealization of the wave surface profile and the wave kinematics given by an appropriate wave theory [7]. The second is the computation of the wave forces on individual members and on the total structure, from the fluid motion.

Two different analysis concepts are used:

- The design wave concept, where a regular wave of given height and period is defined and the forces due to this wave are calculated using a high-order wave theory. Usually the 100-year wave, i.e. the maximum wave with a return period of 100 years, is chosen. No dynamic behaviour of the structure is considered. This static analysis is appropriate when the dominant wave periods are well above the period of the structure. This is the case of extreme storm waves acting on shallow water structures [7].
- Statistical analysis on the basis of a wave scatter diagram for the location of the structure. Appropriate wave spectra are defined to perform the analysis in the frequency domain and to generate random waves, if dynamic analyses for extreme wave loadings are required for deepwater structures. With statistical methods, the most probable maximum force during the lifetime of the structure is calculated using linear wave theory. The statistical approach has to be chosen to analyze the fatigue strength and the dynamic behaviour of the structure [7].

2.2.1 Wave Theory

Wave theories describe the kinematics of waves of water on the basis of potential theory. In particular, they serve to calculate the particle velocities and accelerations and the dynamic pressure as functions of the surface elevation of the waves. The waves are assumed to be long-crested, i.e. they can be described by a two-dimensional flow field, and are characterized by the parameters: wave height (H), period (T) and water depth (d) as shown in Fig. 1.

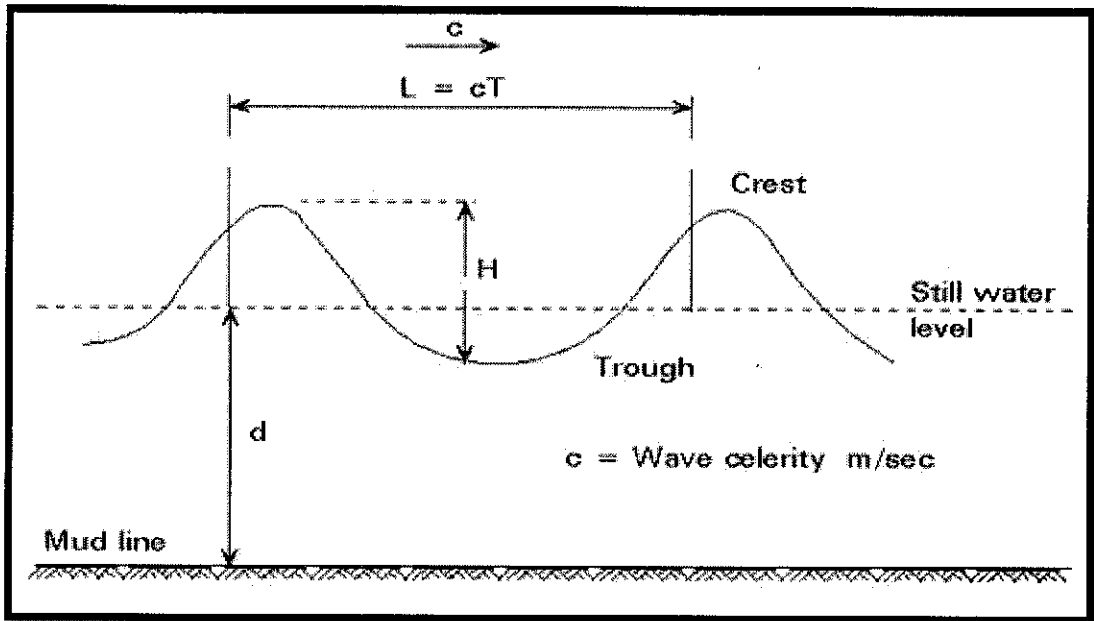


Figure 6: Wave Parameters

Different wave theories of varying complexity, developed on the basis of simplifying assumptions, are appropriate for different ranges of the wave parameters. Among the most common theories are: the linear Airy theory, the Stokes fifth-order theory, the solitary wave theory, the cnoidal theory and Dean's stream function theory [7].

2.2.2 Wave Statistics

In reality, waves do not occur as regular waves, but as irregular sea states. The irregular appearance results from the linear superposition of an infinite number of regular waves with varying frequency. The best means to describe a random sea state is using the wave energy density spectrum $S(f)$, usually called the wave spectrum for simplicity. It is formulated as a function of the wave frequency f using the parameters: significant wave height H_s (i.e. the mean of the highest third of all waves present in a wave train) and mean wave period (zero upcrossing period) T_0 . As an additional parameter, the spectral width can be taken into account [7].

Wave directionality can be introduced by means of a directional spreading function $D(f, \theta)$ where θ is the angle of the wave approach direction. A directional wave spectrum $S(f, \theta)$ can then be defined as:

$$S(f, \theta) = S(f) \cdot D(f, \theta)$$

The response of the structure, i.e. forces and motions are calculated by multiplication of the wave energy spectrum with the square of a linear transfer function. From the resulting response spectrum, the significant and the maximum expected response in a given time interval can be easily deduced.

2.2.3 Wave forces on structural members

Structures exposed to waves experience substantial forces much higher than wind loadings. The forces result from the dynamic pressure and the water particle motions. Two different cases can be distinguished:

- Large volume bodies, termed hydrodynamic compact structures, influence the wave field by diffraction and reflection. The forces on these bodies have to be determined by costly numerical calculations based on diffraction theory [7].
- Slender, hydrodynamically transparent structures have no significant influence on the wave field. The forces can be calculated in a straight-forward manner with Morison's equation. As a rule, Morison equation may be applied when $D/L < 0.2$, where D is the member diameter and L is the wave length [7].

The wave forces on the submerged members can therefore be calculated by Morison equation, which expresses the wave force as the sum of inertia force proportional to the particle acceleration and a non-linear drag force proportional to the square of the particle velocity:

$$F = C_m \frac{\rho \pi D^2}{4} \dot{v} + C_D \frac{\rho D}{2} v |v|$$

where

F is the wave force per unit length on a circular cylinder (N)

v, |v| are water particle velocity normal to the cylinder, calculated with the selected wave theory at the cylinder axis (m/s)

\dot{v} is water particle acceleration normal to the cylinder, calculated with the selected wave theory at the cylinder axis (m/s²)

ρ is the water density (kg/m³)

D is the member diameter, including marine growth (m)

C_D, C_M are drag and inertia coefficients, respectively.

In this form, the equation is valid for fixed tubular cylinders. For the analysis of the motion response of a structure, it has to be modified to account for the motion of the cylinder [13]. The values of C_D and C_M depend on the wave theory used, surface roughness and the flow parameters. According to API-RP2A, C_D is 0.6 to 1.2 and C_M is 1.3 to 2.0.

2.3 Wind Loads

Wind loads on structures are characterized as dynamic loads because their magnitude, direction, and position varies with time. Wind loadings are stochastic because no two records of wind speed or wind direction resemble one another [8]. Since they are stochastic, wind loads are treated as random processes. Wind loads act on the portion of a platform above the water level, as well as on any equipment, housing, derrick, etc. located on the deck. An important parameter pertaining to wind data is the time interval over which wind speeds are averaged. For averaging intervals less than one minute, wind speeds are classified as gusts. For averaging intervals of one minute or longer they are classified as sustained wind speeds.

2.4 Coherence Function

The Coherence Function is a computed measurement that gives a measure of the linear dependence between two signals as a function of frequency [14]. We make an assumption that the system under test is linear and the resulting measurements are therefore representative of the linear system. Since the measurement represents the relationship between two signals, an excitation point and direction and a response point and direction, the Coherence Function can be used to determine the linearity of both stationary inputs. The Coherence Function calculation is defined by the following equation:

$$\gamma^2(f) = \frac{|G_{xy}(f)|^2}{G_{xx}(f)G_{yy}(f)}$$

Where:

$G_{xy}(f)$ = Cross Power Spectrum between the excitation and response signal

$G_{xx}(f)$ = Power Spectrum of the excitation signal

$G_{yy}(f)$ = Power Spectrum of the response signal

f = frequency

The first thing to notice about the Coherence Function is that it is a function of frequency. Therefore its value can change depending on the frequency where the Coherence Function is evaluated. Another thing to notice about the Coherence Function is that it is a 'real' valued function since the numerator is the magnitude squared of the Cross Power Spectrum, a 'real' valued spectrum, and the denominator is the product of the Input (Force) Power Spectrum and the Response (Acceleration) Power Spectrum, both of which are 'real' valued spectrums. Therefore the division of these 'real' valued spectrum results in the Coherence Function being a 'real' valued spectra.

2.4.1 Interpretation of Coherence Function

The Coherence Function γ^2 , when evaluated at a specific frequency, can be interpreted in a similar fashion as the square of the Correlation Coefficient r . The value of the Coherence Function γ^2 at any frequency can have a range of values between 0 (zero) and 1 (one). When the Coherence Function value is 1 there is a perfect linear relationship between the two signals of force and acceleration. When the Coherence Function is 0 there is no relationship between the two signals [14].

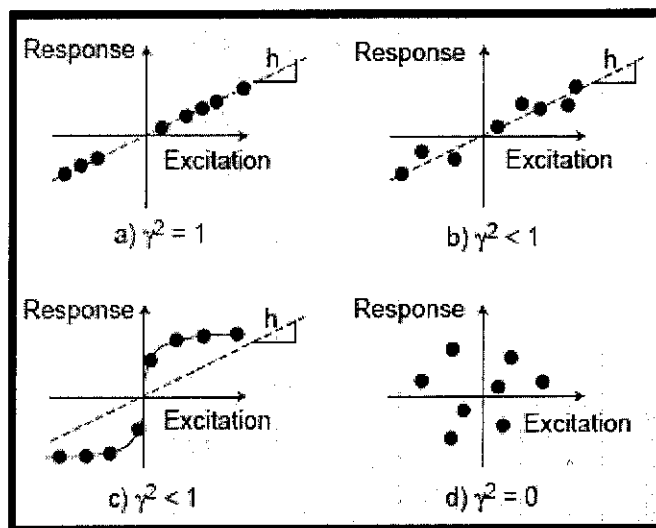


Figure 7: Coherence Function value

Figure 8 illustrates various Coherence Function values for different relationships that might exist between an excitation force and the corresponding response acceleration at a particular frequency. Each dot in Figure 8 represents the input/output relationship for one of the constituents used to compute the average FRF measurement. The slope of the curve is actually the magnitude of the FRF measurement. In Figure 8a there is a perfect linear relationship between the excitation force and response acceleration therefore $\gamma^2 = 1$. In Figure 8b there appears to be a somewhat linear relationship with random spread due to added noise, which causes the γ^2 to be < 1 . Figure 8c similarly shows the γ^2 to be < 1 but now it's due to a nonlinear relationship between the systems excitation and response. Finally in Figure 8d there is no relationship whatsoever between the excitation and response and therefore $\gamma^2 = 0$ [14].

2.4.2 Noise reduction by using Coherence Function

When we are taking the data for computation of the coherence function, noise and lag will appears in both inputs and outputs. As this can be explain due to the reasons why the coherence function is not equal to unity as we compute the value:

- Presence of uncorrelated noise for one or both signals.
- A true nonlinear relation between the excitation and response.
- Errors in Fast Fourier Transform (FFT) when analyzing non periodic.
- Time delays between the excitation and the response signals.

Theoretically the impulse response can be obtained by inverse Fourier transforming the transfer function of the system, $H(j\omega)$ deduced by the expression: $H(j\omega)=Y(j\omega)/X(j\omega)$, where the caps indicate the Fourier transforms. Two main problems are: the presence of poles and zeros of $X(j\omega)$ and $Y(j\omega)$ causes the expression of $H(\omega)$ to be indeterminate, furthermore the noise on both the input and the output has a significant effect where $X(j\omega)$ and $Y(j\omega)$ assume low values [17]. There were many approaches for deconvolution were developed for various field, some of these operate in the frequency domain and consist in the optimization of a filter $F(j\omega)$ in order to reduce the noise effect and to interpolate $H(j\omega)$ where it is indeterminate, the frequency response is estimated by the expression:

$$F(j\omega) = \frac{Y(j\omega)}{X(j\omega)} H(j\omega)$$

It is based on the coherence function used to quantify the ratio between signal and noise. No additional measurements or assumptions on the noise frequency spectrum are required. The proposed criterion might present same advantages in analyzing instantaneous value of the system step response.

2.4.3 Multivariate Coherence Function

Multivariate coherence function shows that the variable of the magnitude square function is multiple. The conventional magnitude-squared coherence function (MSC) between two jointly stationary random processes, $x(t)$ and $y(t)$, is defined as:

$$\gamma^2(f) = \frac{|G_{xy}(f)|^2}{G_{xx}(f)G_{yy}(f)}$$

where $G_{xy}(f)$, $G_{xx}(f)$ and $G_{yy}(f)$ are the theoretical cross and autospectral densities, respectively, at frequency f . The MSC can be estimated by ensemble averaging over various data segments, or by band averaging over adjoining frequency components by a suitable spectral window, of the sample spectra to yield estimate C^2 of γ^2 . Both the MSC and its estimators are bounded by zero and unity. The MSC is a very useful indicator of various properties of the linear relationship between $x(t)$ and $y(t)$, that is, of the coherent common power between the two measured signals [16]. However, it is relatively well known that the estimators are biased estimators. For example, for the case of smoothing by ensemble averaging, and assuming there to be no bias due to a misalignment, it is shown that the bias of C^2 is given by:

$$B(C^2) = E[C^2] - \gamma^2 \sim \frac{1}{N} (1 - \gamma^2)^2 \left(1 - \frac{2\gamma^2}{N}\right)$$

where γ^2 is the theoretical MSC, C^2 is the estimated MSC, and N is the number of time data segments employed. The estimator C^2 of MSC γ^2 does not possess a probability distribution function (PDF) that has a normal (Gaussian) form, thus confidence limits and other statistical descriptors cannot be easily calculated.

2.4.4 Cross-spectrum

The purpose of cross-spectral analysis is to learn how the variability of two time series is interrelated in the spectral domain that is to determine the time scales on which variability is related as well as the characteristic of that covariation [12]. Let say there is two set of time-series of x_t and y_t , the cross-spectrum denoted G_{xy} is actually the product of Fourier Transform for the cross correlation of these two time series:

$$G_{xy} = F |\Gamma_{xy}|(f)$$

Same goes to the power spectrum of the excitation of every signal of time-series x_t and y_t . The power spectrum is the Fourier Transform of the autocorrelation of for both sihnals x_t and y_t , which can be describes as:

$$G_{yy} = F |\Gamma_{yy}|(f)$$

$$G_{xx} = F |\Gamma_{xx}|(f)$$

The cross-spectrum is generally a complex valued function since the cross-covariance function is, neither strictly symmetric nor anti-symmetric. It actually can be defined as the summation of the real quantity and the imaginary quantity:

$$G_{xy} = \Delta_{xy}(f) + i \psi_{xy}(f)$$

where Δ_{xy} is denoted as cospectral which represents the real parts and ψ_{xy} is denoted as quadrature spectrum which represents the imaginary parts. On the other hand, cross-spectrum also can be written in polar coordinates as:

$$G_{xy} = A_{xy}(f)e^{i\phi_{xy}(f)}$$

where A_{xy} is the amplitude spectrum and ϕ_{xy} is the phase spectrum for respective frequency. The amplitude spectrum in this case is actually describes the amplitude as the function of distribution frequency, while the phase spectrum shows which signal occurs first and which signal is delayed. This can be applied in the structure system of considering wind and waves as the input signals, where we are able to determine the lead and delay forces in the specific frequency.

CHAPTER 3

METHODOLOGY

3.1 Method used

The methodology that will be performed throughout the project will be the fraction of time-series basis, which is the amplitude domain analysis, time domain analysis and frequency domain analysis. However, the coherence function analysis will be covered under the frequency domain analysis for the results obtain later. We assumed the linear system to be stationary. A goal of time-series analysis in the frequency domain is to reliably separate periodic oscillations from the random and aperiodic fluctuations [3].

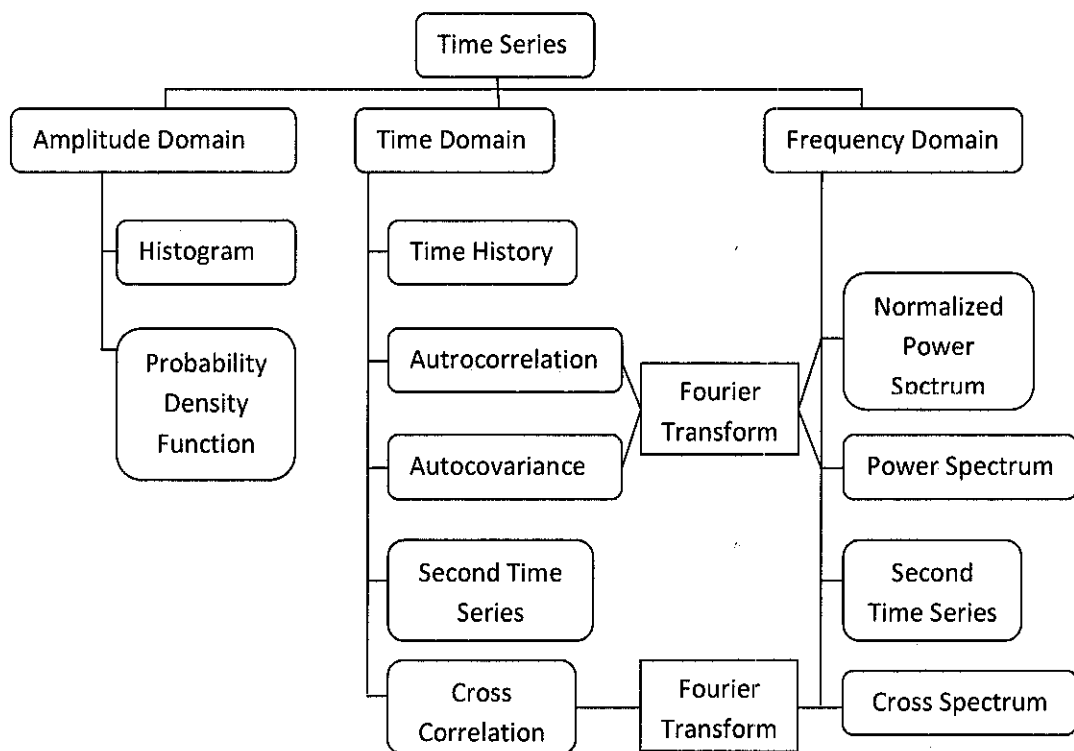


Figure 8: Time Series Analysis

3.1.1 Amplitude Domain

Amplitude domain analysis is an analysis that represents the magnitude of change in the oscillating variable with each oscillation within an oscillating system. One of the examples that based on amplitude domain is histogram. Histogram is a graphical representation, showing a visual impression of the distribution of data. It is an estimate of the probability distribution of a continuous variable.

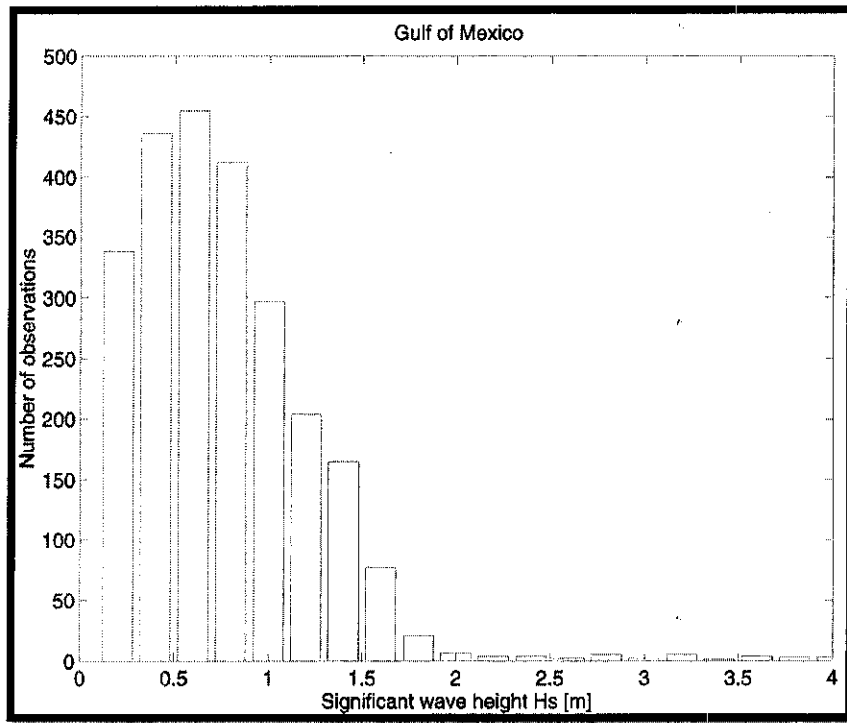


Figure 9: Histogram of significant wave height at Gulf of Mexico

On the other hand, probability density function also one of the amplitude domain analysis. It is a function that describes the relative likelihood for this random variable to occur at a given point. The probability for the random variable to fall within a particular region is given by the integral of this variable's density over the region. The probability density function is nonnegative everywhere, and its integral over the entire space is equal to one.

3.1.2 Time Domain

Time domain is a term used to describe the analysis of mathematical functions, physical signals or time series of economic or environmental data, with respect to time. In the time domain, the signal or function's value is known for all real numbers, for the case of continuous time, or at various separate instants in the case of discrete time.

As to complete the project, the data appears in time series because it is taken from time to time continuously. The inputs data for the system are wind, wave and current. Therefore the method of cross-correlation is necessary to be performed to measure the similarity of two wave forms from the time series as a function of time-lag applied to it. All the paras data is in form of time domain, thus the linear association between two pair of time series are able to be determined.

Whilst for the individual power spectrum, it will be analyze using auto-correlation to obtain the similarity with the same wave form for finding the repeating patterns, such as the presence of periodic signal that is buried under the noise.

3.1.3 Frequency Domain

Later on the time series will be generated into a form of frequency-energy density plot, through Fast Fourier Transform method. It is a term used to describe the domain for analysis of mathematical functions or signals with respect to frequency, rather than time. Frequency-domain analysis is a way of processing interferograms to obtain surface profiles. Frequency domain graph shows how much of the signal lies within each given frequency band over a range of frequencies.

In order to apply Coherence Function as the mechanism tool, the inputs have to be generated to power spectrum individually. By computing the autocorrelation function of the wave profile, then it is valid for us to use Fourier Transform to yield the energy density spectrum or individual power spectrum. Fourier Transform is a time frequency signal analysis that decomposes a signal into its constituent frequencies and smooth the spectrum that appears in ragged edge. Then we are able to use the coherence function formula to obtain the magnitude square the data.

3.2 Software used

3.2.1 Microsoft Excel

Microsoft Excel is a commercial spreadsheet application. It features calculation, graphing tools, pivot tables, and a macro programming language called Visual Basic for Applications. I use this software from the beginning of the project which is collecting data, until the end which is the analysis.

3.2.2 PASW 18 Statistic computer software

PASW is the main software that will be used to analyse the data collected since it has all the function to simplify the process.

3.3 Activities

3.3.1 Gantt Chart

No	Detail / Week	1	2	3	4	5	6	7	8	9	10	11	12	13	14	15
1	Project Works Continue	■	■	■	■	■	■	■								
2	Submission of Progress Report								■							
3	Project Work Continues								■	■	■	■	■			
4	Pre-EDX										■					
5	Submission of Draft Report											■				
6	Submission of Dissertation Draft												■			
7	Submission of Technical Paper													■		
8	Oral Presentation														■	
9	Submission of Project Dissertation															■

Figure 10: FYP2 Gantt Chart

3.3.2 Milestone

No	Items	Week													
		1	2	3	4	5	6	7	8	9	10	11	12	13	14
1	Progress Report Submission								●						
2	Poster Presentation											●			
3	Technical Paper Submission													●	
4	Dissertation Draft													●	
5	Oral Presentation														●
6	Dissertation Submission														●

Figure 11: FYP2 Milestone

CHAPTER 4

RESULTS AND DISCUSSION

4.1 Coherency for Seasonal Pattern

4.1.1 Dulang B Platform (PMO)

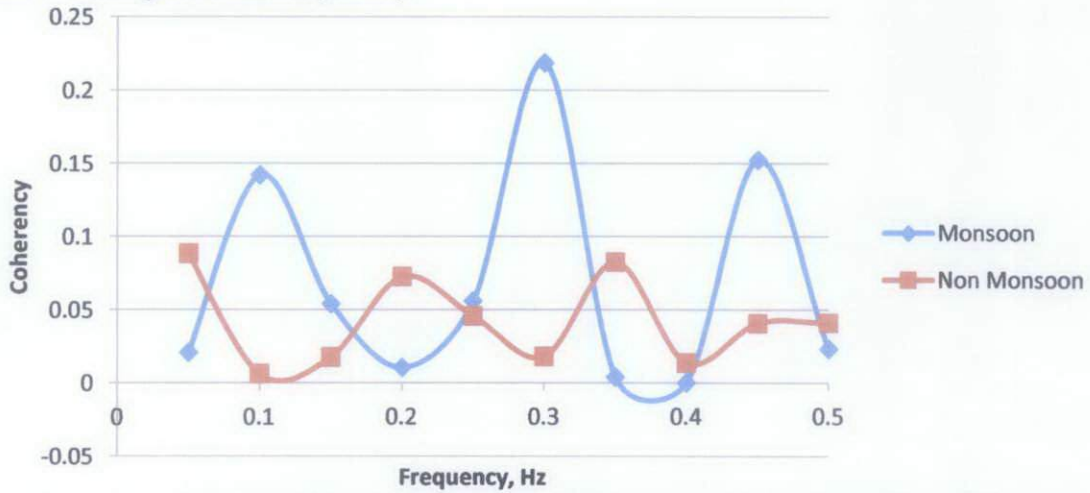


Figure 12: Coherence Function of Wind and Waves for Dulang B Platform in 2000

Frequency, Hz	Monsoon	Non Monsoon
0.05	0.020747	0.088297
0.10	0.141974	0.006036
0.15	0.054182	0.017512
0.20	0.010427	0.0726
0.25	0.056075	0.045792
0.30	0.218561	0.017915
0.35	0.003968	0.082554
0.40	0.000102	0.013515
0.45	0.15232	0.040692
0.50	0.022969	0.040942

Table 4: Coherence Function Table of Wind and Waves for Dulang B Platform in 2000

Based on Figure 12, the coherency clearly shows three dominant wind and waves interaction which peaks at 0.1Hz, 0.3Hz and 0.45Hz. However the highest coherence is at 0.3Hz which valued 0.22. The seasonal pattern shows that during monsoon season, the interaction of wind and waves are more linear compared to non monsoon season from the maximum coherency range between both seasons. The optimum joint interaction for non monsoon also peaks at different frequency compared to monsoon season which at 0.5Hz, 0.2Hz and 0.35Hz. Clearly we can say that the coherency graph for non monsoon season is shifted more to the left, in means toward lower frequency of more non linear interaction between wind and waves during this season.

4.1.2 Samarang Platform (SBO)

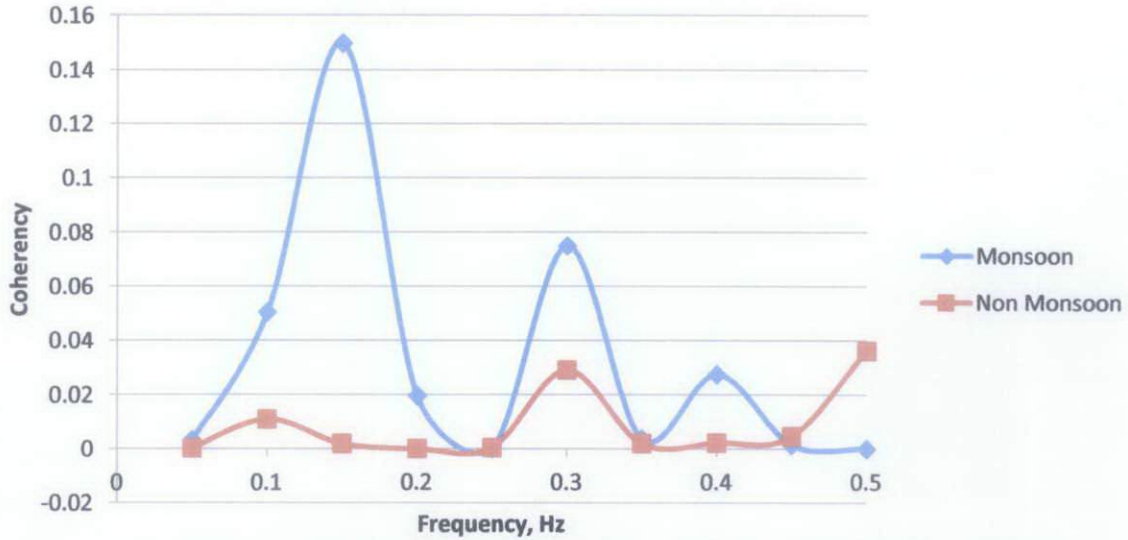


Figure 13: Coherence Function of Wind and Waves for Samarang Platform in 2000

Frequency, Hz	Monsoon	Non Monsoon
0.05	0.00328	0.000146
0.10	0.050449	0.010947
0.15	0.149766	0.001908
0.20	0.019554	4.32E-05
0.25	8.03E-05	0.000417
0.30	0.0749	0.028993
0.35	0.003723	0.001973
0.40	0.02744	0.002179
0.45	0.0015	0.004667
0.50	3.75E-05	0.036109

Table 5: Coherence Function Table of Wind and Waves for Samarang Platform in 2000

Figure 13 also shows the similar seasonal pattern from Figure 12 where the coherency value during monsoon season has more linear relationship compare to non monsoon season. In addition, the dominant peaks are at frequency 0.15Hz, 0.3Hz and 0.4Hz. The interaction of wind and waves shows a significant optimization at 0.15Hz valued 0.15 of coherency. This result also explains that the maximum value of coherence is corresponded to 6 seconds wave period where the interaction is optimum. However the seasonal pattern during non monsoon shows a true non linear relationship between wind and waves since most of the coherency valued almost zero at every frequency and the slightly value near to zero can be assume as negligible. The fluctuation pattern of coherency for Samarang and Dulang B are actually shows similarity but differs in range of coherency.

4.1.3 Tukau Platform (SKO)

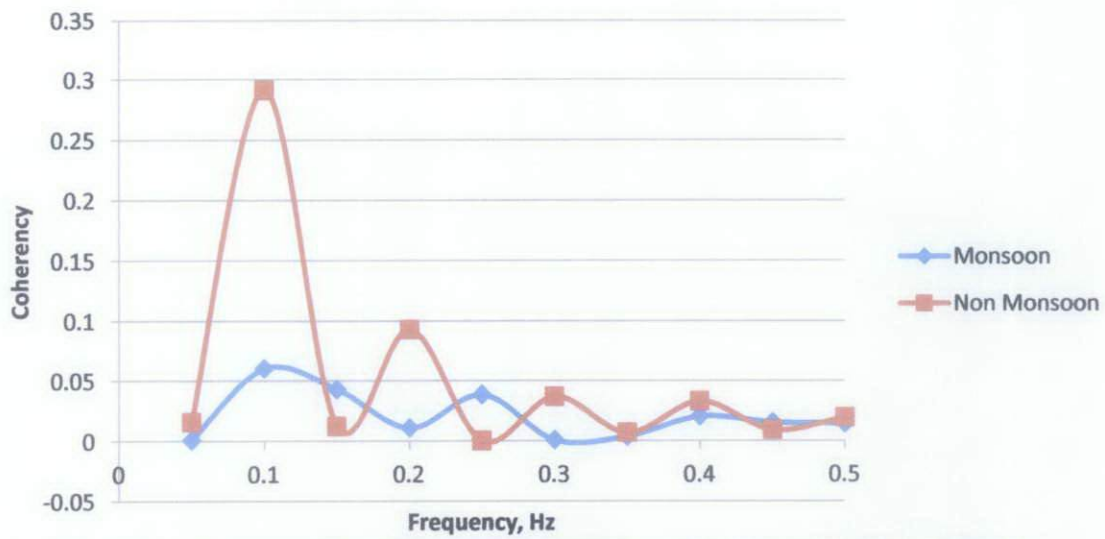


Figure 14: Coherence Function of Wind and Waves for Tukau Platform in 2000

Frequency, Hz	Monsoon	Non Monsoon
0.05	0.000675	0.015678
0.10	0.060392	0.291289
0.15	0.042955	0.012347
0.20	0.010874	0.092635
0.25	0.03857	0.000205
0.30	0.000856	0.036863
0.35	0.003843	0.006889
0.40	0.020466	0.032963
0.45	0.015565	0.009212
0.50	0.014594	0.019469

Table 6: Coherence Function Table of Wind and Waves for Tukau Platform in 2000

Refers to Figure 14, it shows a very different seasonal pattern compared to PMO and SBO. The joint interaction between wind and waves shows more linear relationship during non monsoon season instead of monsoon season. Especially at frequency 0.1Hz, the coherency value peaks till 0.3 which is the highest value during non monsoon season if we refer to Figure 15 that will be discussed in the second part of result. During the monsoon season, the joint interaction between wind and waves can be considered as non linear relationship since the coherence value is almost zero. The results prove that the environmental condition at Tukau is indirectly proportion to operation field patterns of Dulang B and Samarang. Tukau is believed to have a shielding effect due to its location of operation. The factor that is possibly leads to this finding will be the environmental condition which is the water depth and also the river effect.

4.2 Coherency for Different Operation Field

4.2.1 Monsoon Season

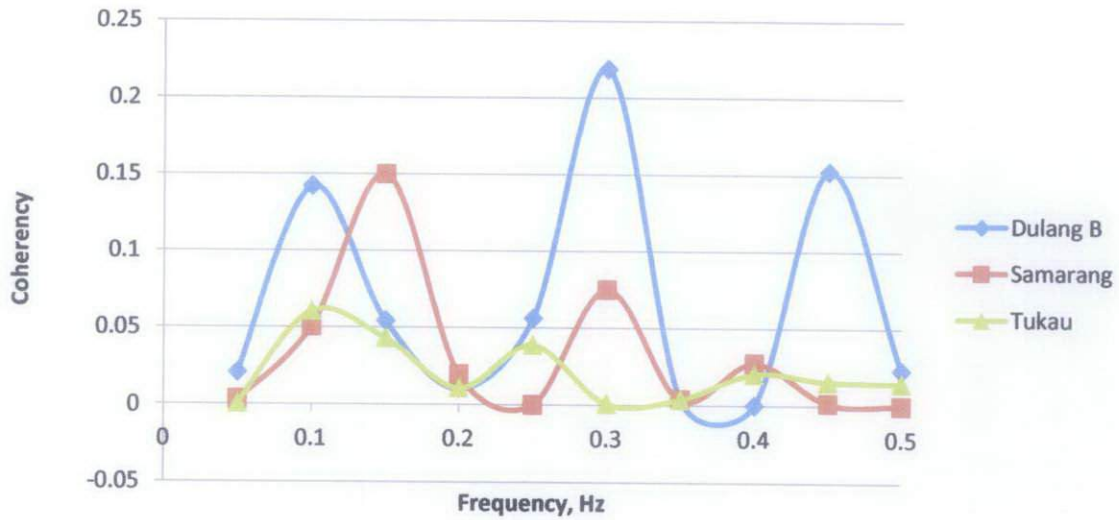


Figure 15: Coherence Function of Wind and Waves during Monsoon Season in 2000

Frequency, Hz	Dulang B	Samarang	Tukau
0.05	0.020747	0.00328	0.000675
0.10	0.141974	0.050449	0.060392
0.15	0.054182	0.149766	0.042955
0.20	0.010427	0.019554	0.010874
0.25	0.056075	8.03E-05	0.03857
0.30	0.218561	0.0749	0.000856
0.35	0.003968	0.003723	0.003843
0.40	0.000102	0.02744	0.020466
0.45	0.15232	0.0015	0.015565
0.50	0.022969	3.75E-05	0.014594

Table 7: Coherence Function Table of Wind and Waves during Monsoon Season in 2000

Based on Figure 15, we can see that the seasonal pattern during monsoon for Dulang B and Samarang has similarity, except Tukau. The similar patterns are the frequencies where the coherency optimum and also the number of peaking. The relationship of wind and waves interaction at Tukau shows almost non linear relationship since the coherency valued below 0.1 for every frequency. Despite the similarity shows for Dulang B and Samarang, Dulang B shows the highest linearity of wind and waves relationship at frequency of 0.3Hz. While Samarang shows maximum linear relationship at frequency 0.15Hz that is slightly significance since it the value is 0.15, which we can categorized as the same interaction of environmental condition at PMO for the specific frequency.

4.2.2 Non Monsoon Season

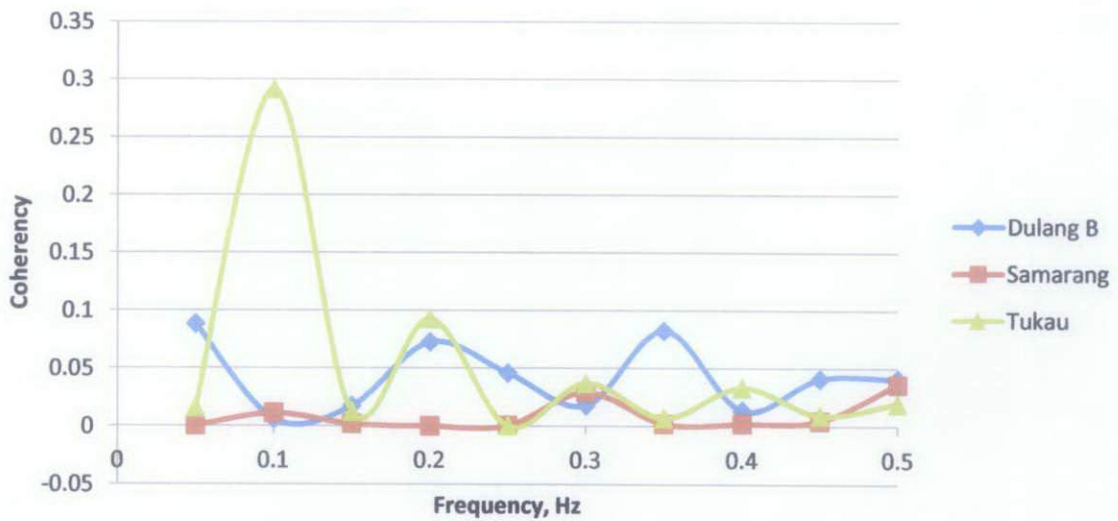


Figure 16: Coherence Function of Wind and Waves during Non Monsoon in 2000

Frequency, Hz	Dulang B	Samarang	Tukau
0.05	0.088297	0.000146	0.015678
0.10	0.006036	0.010947	0.291289
0.15	0.017512	0.001908	0.012347
0.20	0.0726	4.32E-05	0.092635
0.25	0.045792	0.000417	0.000205
0.30	0.017915	0.028993	0.036863
0.35	0.082554	0.001973	0.006889
0.40	0.013515	0.002179	0.032963
0.45	0.040692	0.004667	0.009212
0.50	0.040942	0.036109	0.019469

Table 8: Coherence Function of Wind and Waves during Non Monsoon in 2000

Refers to Figure 16, Tukau shows a significant value of coherency at frequency 0.1Hz, which makes it stand out obviously from other operation field for the interaction of wind and waves. The coherency also is recorded as the highest compare to all the results that we obtained, which valued 0.3. The coherency decrease proportionally to the right side of the frequency. Although the interaction of wind and waves maximum at this frequency, the respective wave action is categorized as calm state since it is 10 second wave period. The environmental condition at PMO and SBO during non monsoon season shows a true non linear relationship of wind and waves as the coherency shows not significance value. The value is very small, that correspond to a slightly interaction of wind and waves together.

CHAPTER 5

RECOMMENDATIONS

First of all, it is recommended to do the research and analysis on these three platforms because we are able to distinguish the real environmental condition with the respective location. Although it operates at the same sea which is the South China Sea, each platform is exposed the undetermined nature forces due to its latitude and longitude. Therefore the probability of dissimilar force occurrence is expected.

Besides, it is recommended to check the raw data available that is collected from the respective platform before any analysis is done. This is because the data might have instrumentals error that will leads to difficulties in computing the coherence function calculation and also difficulties in using the mathematical software. The set of metocean data needs to go through for a thorough checking so that it is valid for further analysis.

For further thorough analysis regarding the climate and environmental condition towards platform structure, it is recommended to do researches that include more than one platform in the specific operation field region. This is to ensure the result obtained is more accurate to describe the environmental condition at specific operation region. The assumption for one platform that represents one operation field region is negligible since the field operation coverage is very wide.

Besides, a long period of studies need to be considered which will include the hurricane event and other extreme event so that a proper criteria or standards can be performed and implied in the operation sector as well as the platform designing stage. This vase spectral analysis can provide us more understanding of the environmental action and give us the opportunity for any improvements required by broaden the scope of study in means extending the studies duration. The measured data however is very crucial to be recorded errors-free or less error so that the outcomes in the end are valid.

CHAPTER 6

CONCLUSION

As the conclusion, this project is somehow relatively important as researches for offshore structure studies. The results obtained might be able to help to improve the conservative approach of structure designing and recommendation for *Structural Integrity Management System* (SIMS) which is practiced by PETRONAS recently. After all, more researches need to be done in order to yield high accuracy results and wise interpretation of data is made.

Based on all the outcomes obtained, we can conclude that the climate seasons and the platform operation field location are actually has a different relationship of wind and waves joint interaction as well as the environmental condition. The results show that wind is only 30% generating the wave and there are other factors which possibly tend to generate wave for particular platforms. For instance, tidal effects, gravity pull by the moon or other parts of the sea.

We found that the interaction of wind and waves at PMO have more linearity during monsoon season. The pattern show that wind is not interacts with wave at certain frequency. It shows that the wave action is volatile compares to non monsoon season. Thus the designing criteria shall consider the respective wave period.

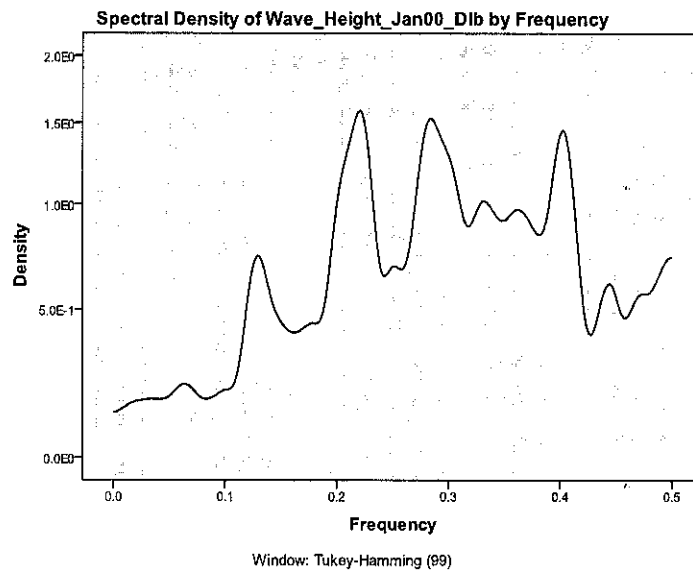
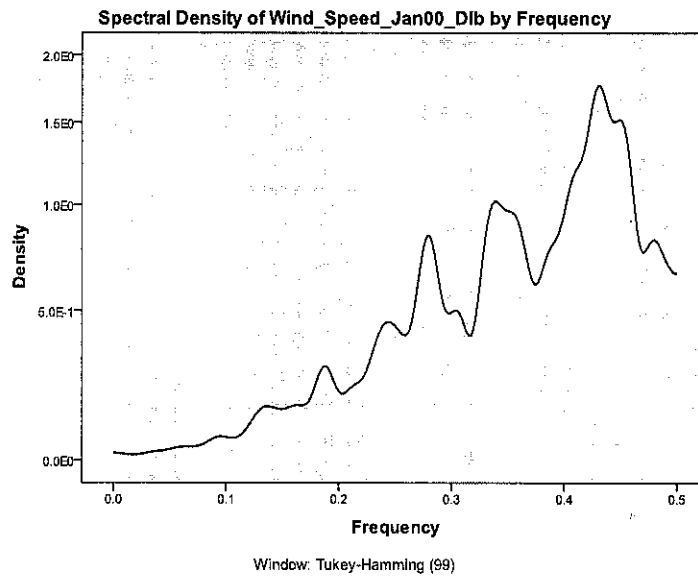
On the other hand, the findings at SBO shows a true non linear relationship of wind and waves during non monsoon season and the wave period of 6 seconds contains the a linear relationship with respected to the wind speed during the monsoon season. The dominant wave action can be categorized as calm as compared to PMO wave action which is 3 seconds wave period.

Lastly, the conclusion that we can make for SKO is that the wind and waves relationship shows a significantly linear relationship during non monsoon season, which optimum at 10 seconds wave period. While the coherency during monsoon season shows a non linear relationship of wind and waves almost for all frequencies.

REFERENCES

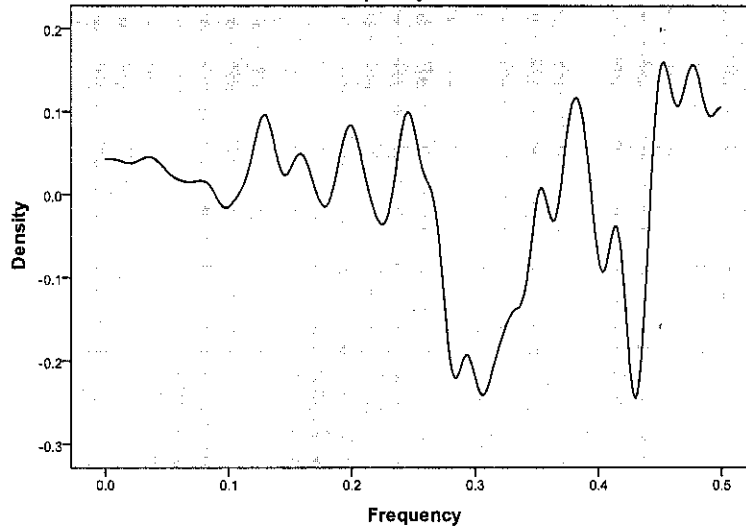
1. Offshore Wind Farms – the Need of Metocean Data; *Vagner Jacobsen and Morten Rugjberg*, DHI Water & Environment.
2. Data Analysis Method in Physical Oceanography; *William J. Emery and Richard E. Thompson*.
3. Hydrodynamics of Offshore Structures; *S.K. Chakrabarti*.
4. Simulation of Joint Wind and Waves Loading Time Histories; *Shane Colwel and Biswajit Basu*, Dublin Institute of Technology, ISSC 2006.
5. Statistical Data Analysis for Ocean and Atmospheric Sciences; *H. Jean Thiebaux*.
6. Design of Fixed Offshore Structure; *Petronas Carigali SDN BHD*, Supplementary to PTS 20.073.
7. Design of Offshore Structures, Chapter 2; *Dr. Kurian V. John*.
8. Statistical Analysis of Wind Loadings and Responses of a Transmission Tower Structure; *Assoc. Prof. Dr Shahir Liew*, A Dissertation in Civil Engineering, 1988.
9. What is Frequency Domain Analysis? ; *P de Groot*, ZYGO R&D Technical Bulletin, 1993.
10. API-RP2A, "Recommended Practice for Planning, Designing and Constructing Fixed Offshore Platforms", American Petroleum Institute, Washington, D.C., 18th ed., 1989.
11. DNV, "Rules for the Design, Construction and Inspection of Offshore Structures", *Det Norske Veritas*, Oslo, 1977 (with corrections 1982).
12. Statistical Analysis in Climate Research; *Han Von Storch, Francis W. Zwiers*.
13. Dynamic Response of Offshore Structures to Extreme Waves including Fluid - Structure Interaction; *Anagnostopoulos, S.A.*, Engr. Structures, Vol. 4, pp.179-185, 1982.
14. What is Coherence Function and How Can it be Used to Find Measurement and Test Setup Problem; *David Formenti*, Sage Technologies, Morgan Hill, California.
15. Structural Integrity Management System for Fixed Offshore Platforms in Malaysia.
16. Transformed Coherence Function for Multivariate Series; *Alan G. Jones*, IEEE Transactions on Acoustic, Speech and Signal Processing, Vol. ASSP-29, No. 2, 1981.
17. Noise Effect Reduction Obtained by Using Coherence Function in Deconvolution; *P. Fiorentin*, IEEE Instrumentation and Measurement Technology Conference Budapest, Hungary, 2001.

Dulang B 2000 – Monsoon Season



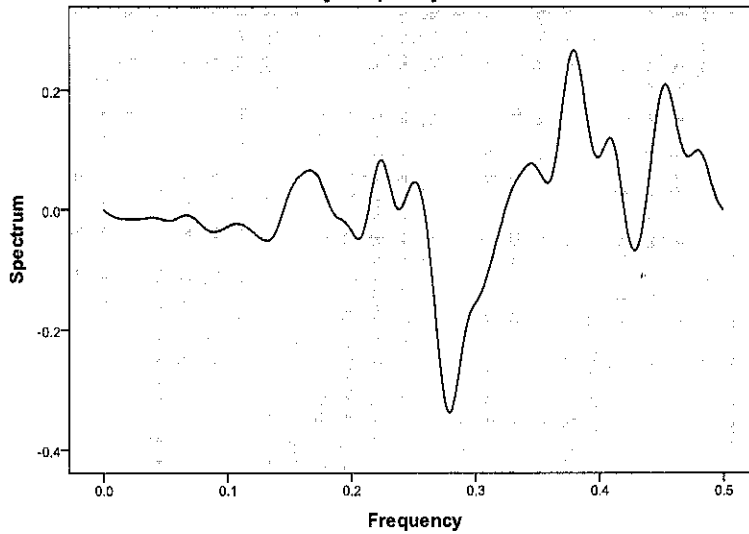
Frequency, Hz	Wind Spectrum, G_{xx}	Waves Spectrum, G_{yy}
0.05	0.0299	0.1816
0.1	0.0638	0.2013
0.15	0.1485	0.4474
0.2	0.2049	0.9968
0.25	0.439	0.6844
0.3	0.4948	1.2881
0.35	0.9661	0.9155
0.4	0.9641	1.4263
0.45	1.5126	0.544
0.5	0.6604	0.7303

Cospectral Density of Wind_Speed_Jan00_Dib and Wave_Height_Jan00_Dib by Frequency



Window: Tukey-Hamming (99)

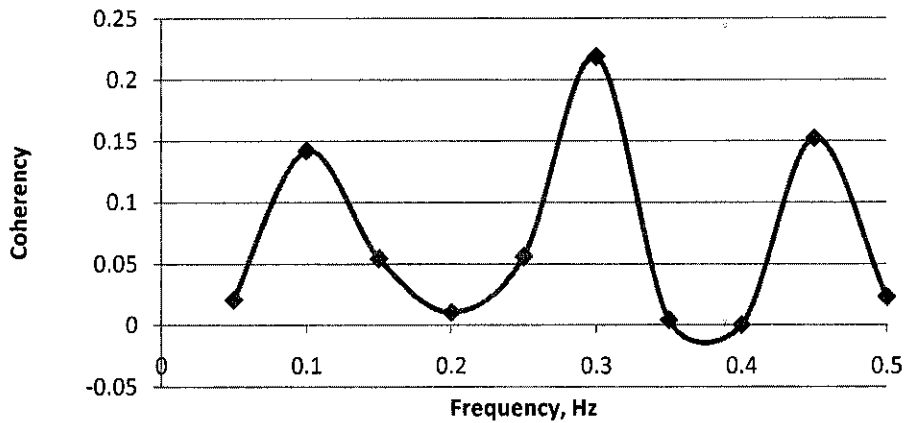
Quadrature Spectrum of Wind_Speed_Jan00_Dib and Wave_Height_Jan00_Dib by Frequency



Window: Tukey-Hamming (99)

Frequency, Hz	Cospectral, Δ_{xy}	Quadrature Spectrum, Ψ_{xy}
0.05	0.0284	-0.018
0.1	-0.0148	-0.02794
0.15	0.0305	0.0295
0.2	0.0824	-0.036
0.25	0.0841	0.0457
0.3	-0.2188	-0.154
0.35	-0.0081	0.0674
0.4	-0.0782	0.0901
0.45	0.1529	0.2011
0.5	0.1052	0

**Coherence Function of Wind and Waves for Dulang B 2000
- Monsoon Season**



Cross Spectrum:

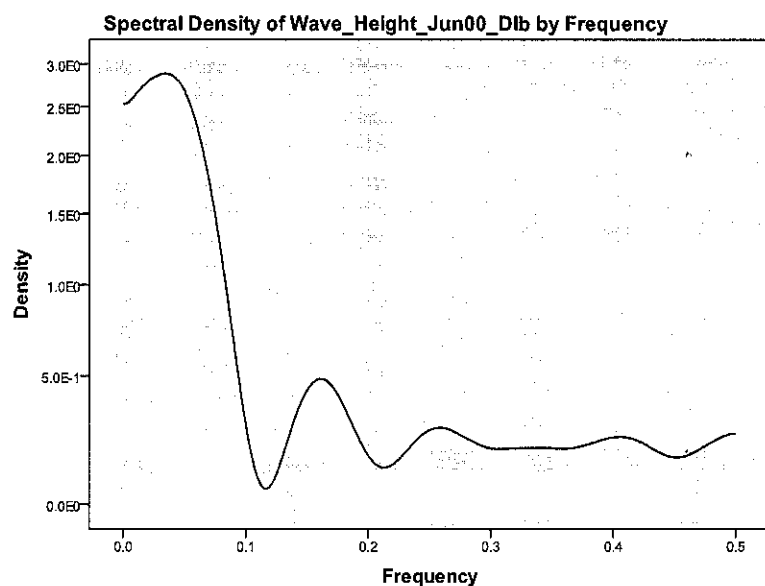
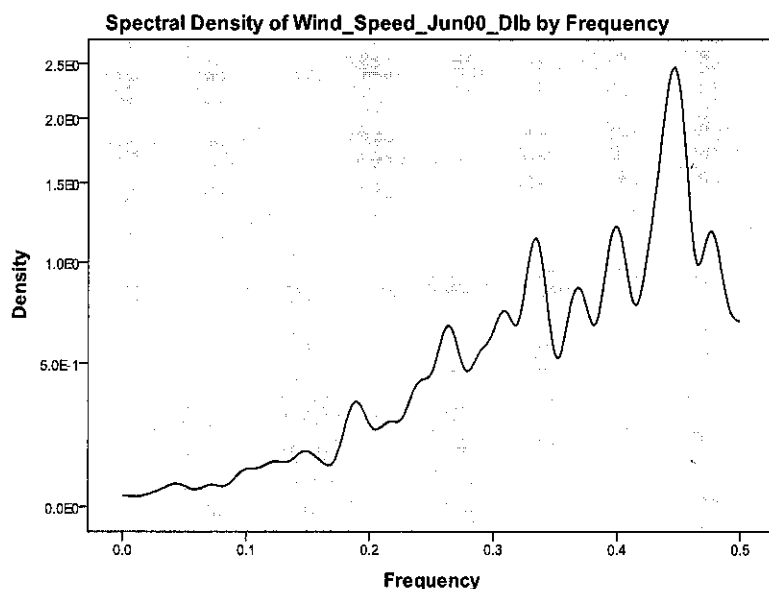
$$G_{xy} = \Delta_{xy}(f) + i \psi_{xy}(f)$$

Coherence Function:

$$\gamma^2(f) = \frac{|G_{xy}(f)|^2}{G_{xx}(f)G_{yy}(f)}$$

Frequency, Hz	Wind Spectrum, G_{xx}	Waves Spectrum, G_{yy}	Cospectral, Δ_{xy}	Quadrature Spectrum, ψ_{xy}	Cross Spectrum, G_{xy}	Coherence, γ_{xy}
0.05	0.0299	0.1816	0.0284	-0.018	0.010612	0.020747
0.1	0.0638	0.2013	-0.0148	-0.02794	-0.04269	0.141974
0.15	0.1485	0.4474	0.0305	0.0295	0.059989	0.054182
0.2	0.2049	0.9968	0.0824	-0.036	0.046154	0.010427
0.25	0.439	0.6844	0.0841	0.0457	0.129796	0.056075
0.3	0.4948	1.2881	-0.2188	-0.154	-0.37324	0.218561
0.35	0.9661	0.9155	-0.0081	0.0674	0.059245	0.003968
0.4	0.9641	1.4263	-0.0782	0.0901	0.011841	0.000102
0.45	1.5126	0.544	0.1529	0.2011	0.354033	0.15232
0.5	0.6604	0.7303	0.1052	0	0.105245	0.022969

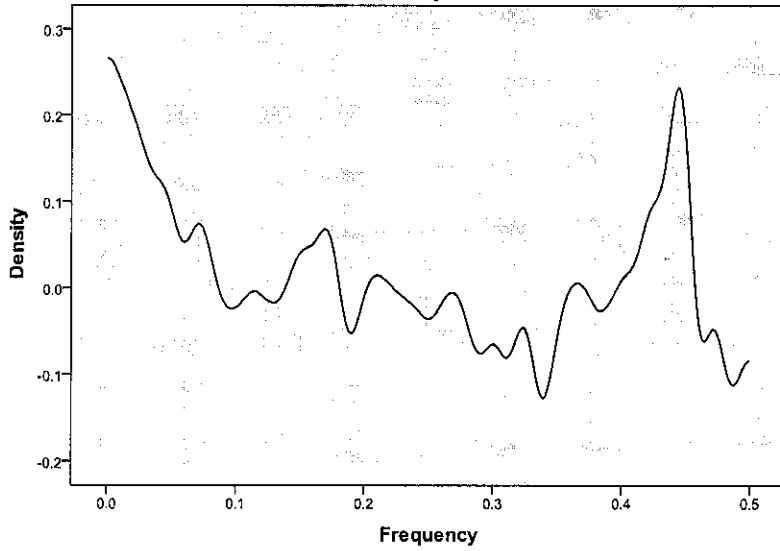
Dulang B 2000 – Non Monsoon Season



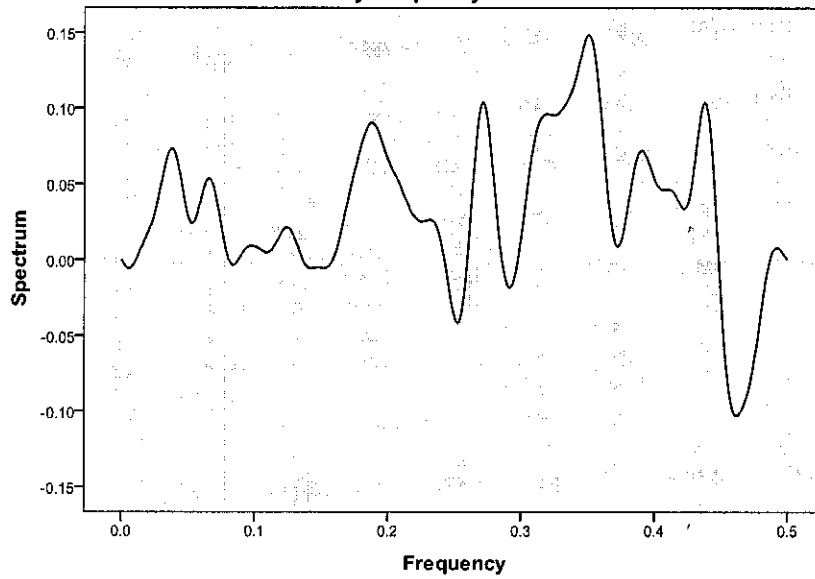
Window: Tukey-Hamming (99)

Frequency, Hz	Wind Spectrum, G_{xx}	Waves Spectrum, G_{yy}
0.05	0.0604	2.6707
0.1	0.1118	0.2837
0.15	0.1677	0.4354
0.2	0.2611	0.165
0.25	0.4604	0.2644
0.3	0.6448	0.1942
0.35	0.5359	0.1945
0.4	1.21	0.2364
0.45	2.2953	0.1609
0.5	0.6913	0.2508

Cospectral Density of Wind_Speed_Jun00_Dlb and Wave_Height_Jun00_Dlb by Frequency



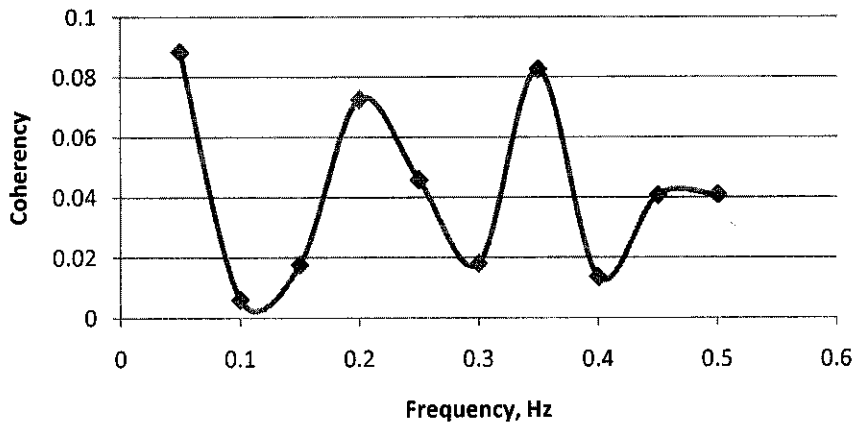
Quadrature Spectrum of Wind_Speed_Jun00_Dlb and Wave_Height_Jun00_Dlb by Frequency



Window: Tukey-Hamming (99)

Frequency, Hz	Cospectral, Δ_{xy}	Quadrature Spectrum, ψ_{xy}
0.05	0.0913	0.0281
0.1	-0.022	0.0087
0.15	0.0412	-0.005
0.2	-0.01	0.0654
0.25	-0.036	-0.039
0.3	-0.065	0.0177
0.35	-0.056	0.1485
0.4	0.0104	0.0518
0.45	0.1568	-0.034
0.5	-0.084	0

**Coherence Function of Wind and Waves for Dulang B 2000
 - Non Monsoon**



Cross Spectrum:

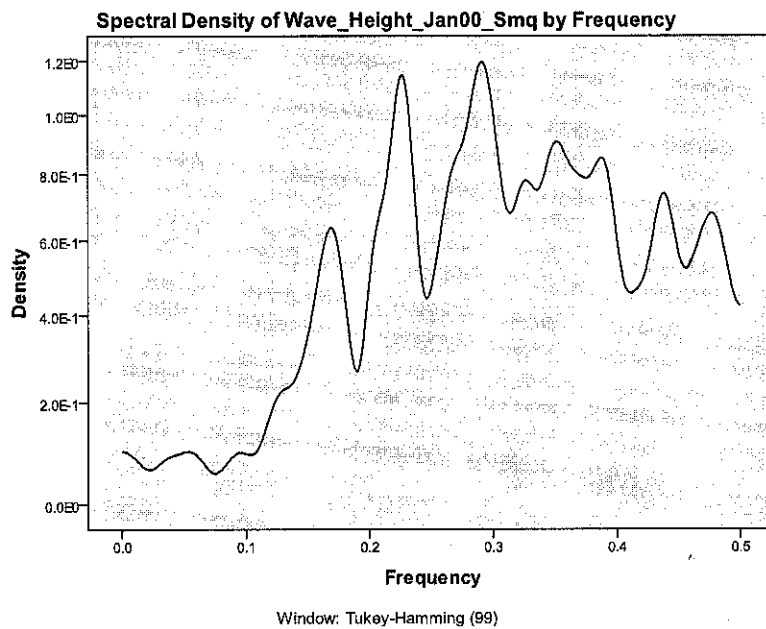
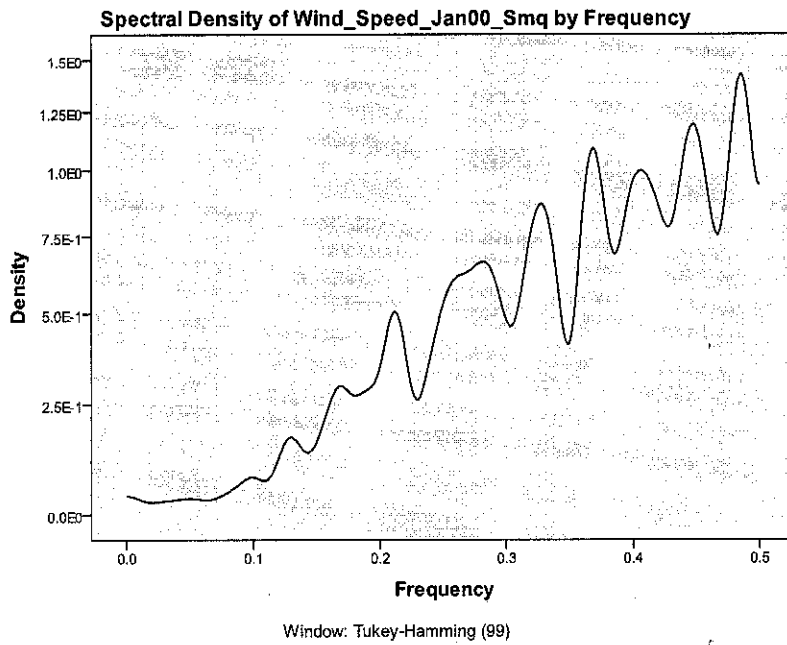
$$G_{xy} = \Delta_{xy}(f) + i \psi_{xy}(f)$$

Coherence Function:

$$\gamma^2(f) = \frac{|G_{xy}(f)|^2}{G_{xx}(f)G_{yy}(f)}$$

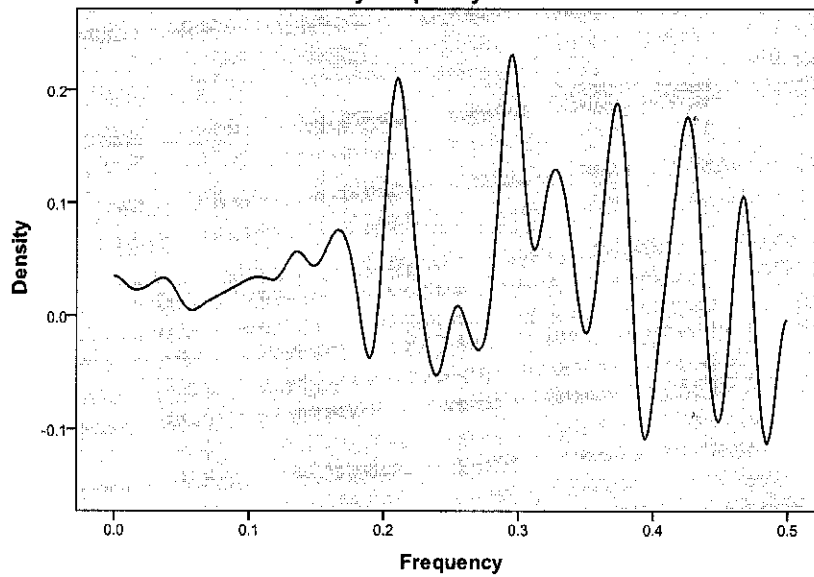
Frequency, Hz	Wind Spectrum, G_{xx}	Waves Spectrum, G_{yy}	Cospectral, Δ_{xy}	Quadrature Spectrum, ψ_{xy}	Cross Spectrum, G_{xy}	Coherence, γ_{xy}
0.05	0.0604	2.6707	0.0913	0.0281	0.119388	0.088297
0.1	0.1118	0.2837	-0.022	0.0087	-0.01383	0.006036
0.15	0.1677	0.4354	0.0412	-0.005	0.035759	0.017512
0.2	0.2611	0.165	-0.01	0.0654	0.055927	0.0726
0.25	0.4604	0.2644	-0.036	-0.039	-0.07466	0.045792
0.3	0.6448	0.1942	-0.065	0.0177	-0.04736	0.017915
0.35	0.5359	0.1945	-0.056	0.1485	0.092765	0.082554
0.4	1.21	0.2364	0.0104	0.0518	0.062173	0.013515
0.45	2.2953	0.1609	0.1568	-0.034	0.122583	0.040692
0.5	0.6913	0.2508	-0.084	0	-0.08424	0.040942

Samarang 2000 – Monsoon Season



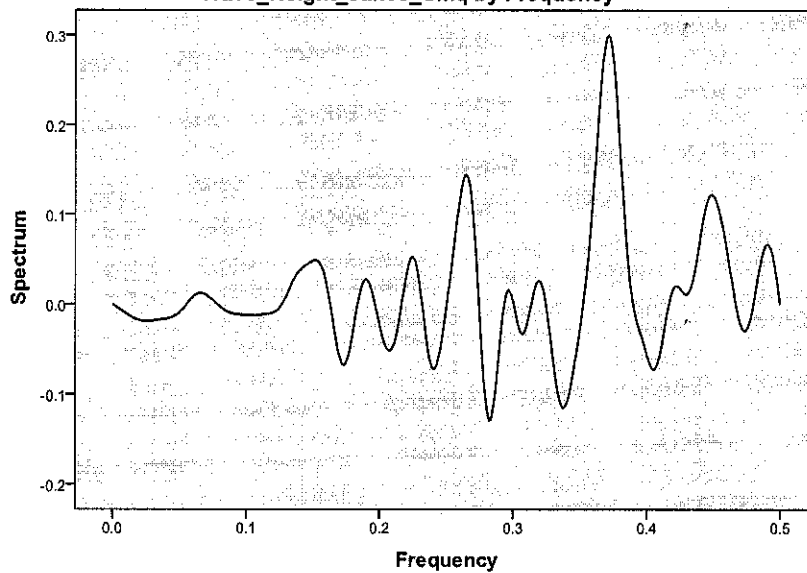
Frequency, Hz	Wind Spectrum, G_{xx}	Waves Spectrum, G_{yy}
0.05	0.0336	0.0992
0.1	0.0793	0.0959
0.15	0.1618	0.3528
0.2	0.3499	0.4974
0.25	0.5306	0.4738
0.3	0.4772	0.9939
0.35	0.422	0.9061
0.4	0.9652	0.5944
0.45	1.167	0.5545
0.5	0.9438	0.4254

Cospectral Density of Wind_Speed_Jan00_Smq and Wave_Height_Jan00_Smq by Frequency



Window: Tukey-Hamming (99)

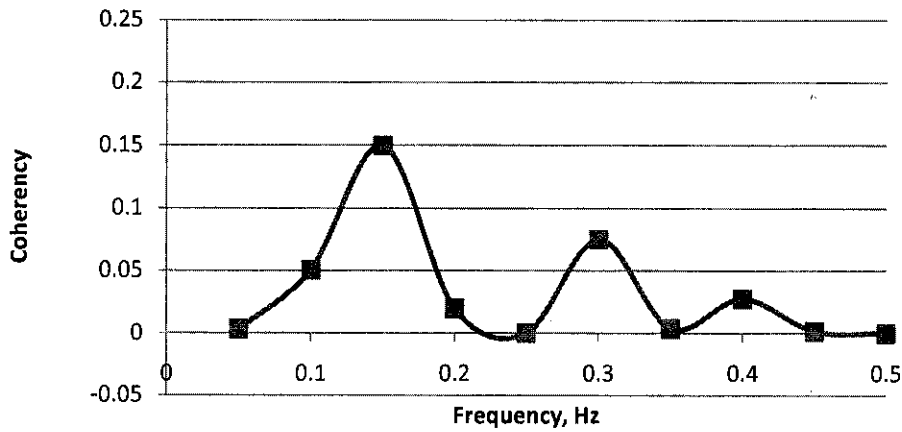
Quadrature Spectrum of Wind_Speed_Jan00_Smq and Wave_Height_Jan00_Smq by Frequency



Window: Tukey-Hamming (99)

Frequency, Hz	Cospectral, Δ_{xy}	Quadrature Spectrum, ψ_{xy}
0.05	0.0128	-0.00946
0.1	0.032	-0.01242
0.15	0.0445	0.047933
0.2	0.0834	-0.0251
0.25	-0.0036	-0.0009
0.3	0.1885	-0.00006
0.35	-0.0156	-0.02214
0.4	-0.0667	-0.05877
0.45	-0.088	0.119164
0.5	-0.004	0

**Coherence Function of Wind and Waves for Samarang 2000
 - Monsoon Season**



Cross Spectrum:

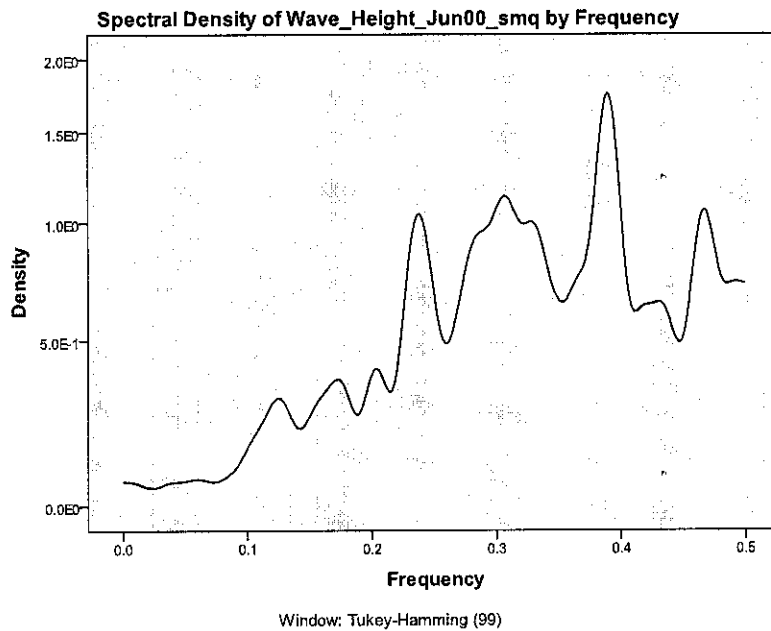
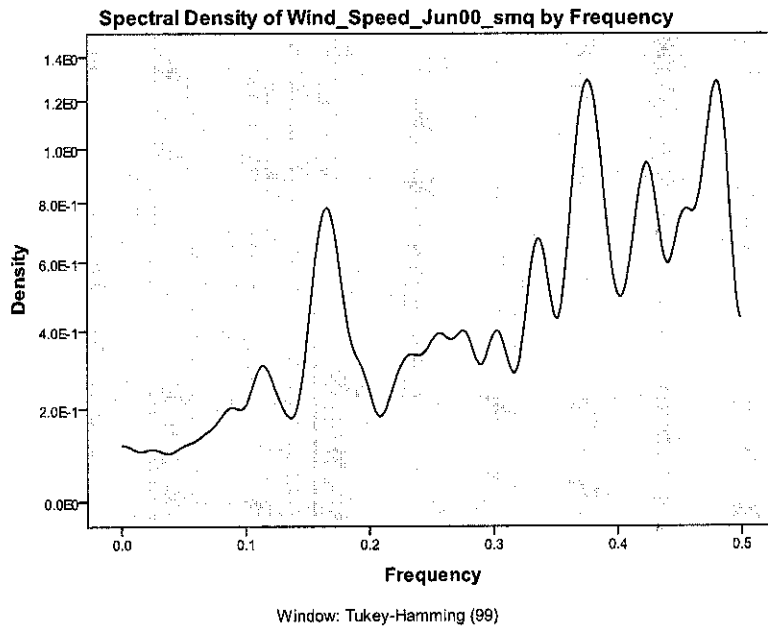
$$G_{xy} = \Delta_{xy}(f) + i \psi_{xy}(f)$$

Coherence Function:

$$\gamma^2(f) = \frac{|G_{xy}(f)|^2}{G_{xx}(f)G_{yy}(f)}$$

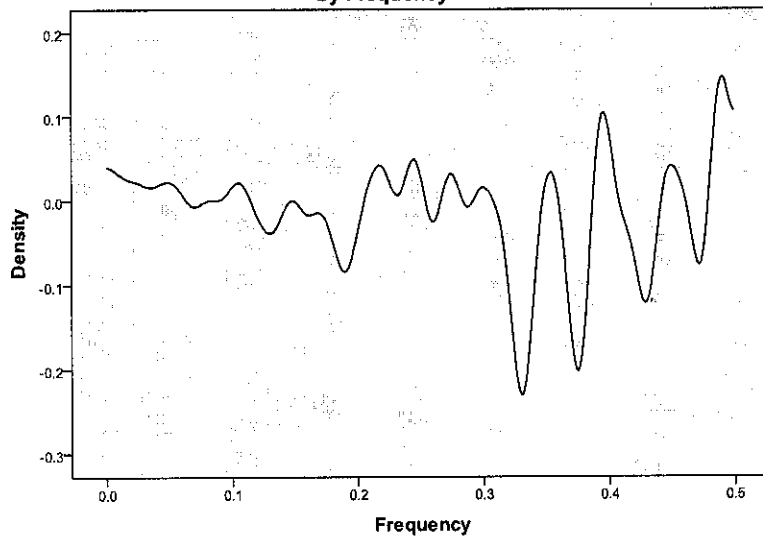
Frequency, Hz	Wind Spectrum, G_{xx}	Waves Spectrum, G_{yy}	Cospectral, Δ_{xy}	Quadrature Spectrum, ψ_{xy}	Cross Spectrum, G_{xy}	Coherence, γ_{xy}
0.05	0.0336	0.0992	0.0128	-0.00946	0.003307	0.00328
0.1	0.0793	0.0959	0.032	-0.01242	0.01958	0.050449
0.15	0.1618	0.3528	0.0445	0.047933	0.092475	0.149766
0.2	0.3499	0.4974	0.0834	-0.0251	0.058333	0.019554
0.25	0.5306	0.4738	-0.0036	-0.0009	-0.00449	8.03E-05
0.3	0.4772	0.9939	0.1885	-0.00006	0.18847	0.0749
0.35	0.422	0.9061	-0.0156	-0.02214	-0.03773	0.003723
0.4	0.9652	0.5944	-0.0667	-0.05877	-0.12547	0.02744
0.45	1.167	0.5545	-0.088	0.119164	0.031155	0.0015
0.5	0.9438	0.4254	-0.004	0	-0.00388	3.75E-05

Samarang 2000 – Non Monsoon Season



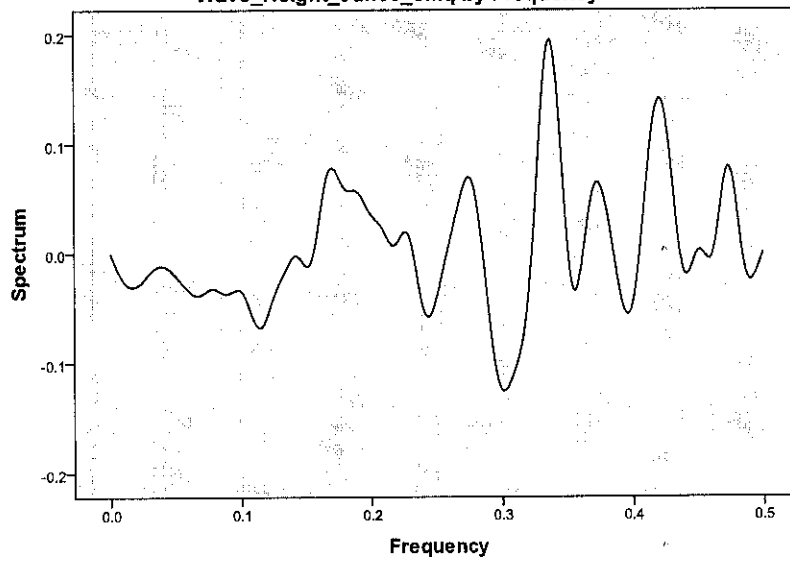
Frequency, Hz	Wind Spectrum, G_{xx}	Waves Spectrum, G_{yy}
0.05	0.1158	0.0629
0.1	0.2102	0.1545
0.15	0.4022	0.2483
0.2	0.2391	0.3827
0.25	0.3729	0.6766
0.3	0.3937	1.0753
0.35	0.4348	0.6516
0.4	0.5015	1.0366
0.45	0.7443	0.5223
0.5	0.435	0.7218

Cospectral Density of Wind_Speed_Jun00_smq and Wave_Height_Jun00_smq by Frequency



Window: Tukey-Hamming (99)

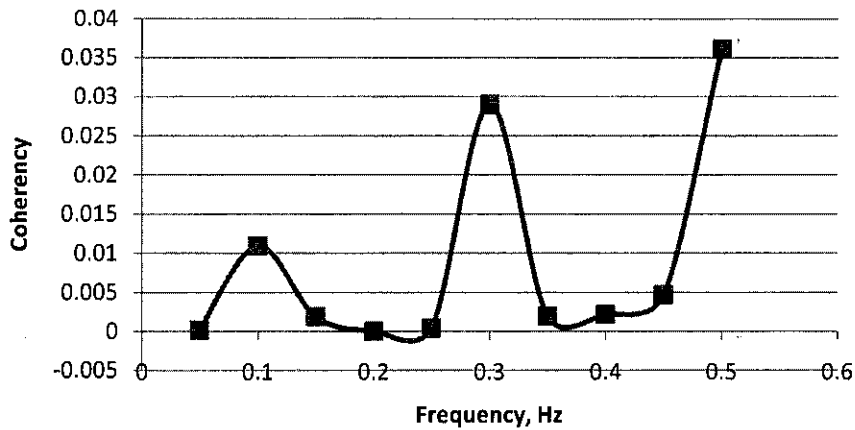
Quadrature Spectrum of Wind_Speed_Jun00_smq and Wave_Height_Jun00_smq by Frequency



Window: Tukey-Hamming (99)

Frequency, Hz	Cospectral, Δ_{xy}	Quadrature Spectrum, Ψ_{xy}
0.05	0.0219	-0.021
0.1	0.0162	-0.035
0.15	-0.002	-0.012
0.2	-0.036	0.0336
0.25	0.0276	-0.038
0.3	0.0149	-0.126
0.35	0.0248	-0.001
0.4	0.0751	-0.041
0.45	0.0405	0.0021
0.5	0.1065	0

**Coherence Function of Wind and Waves for Samarang 2000 -
 Non Monsoon**



Cross Spectrum:

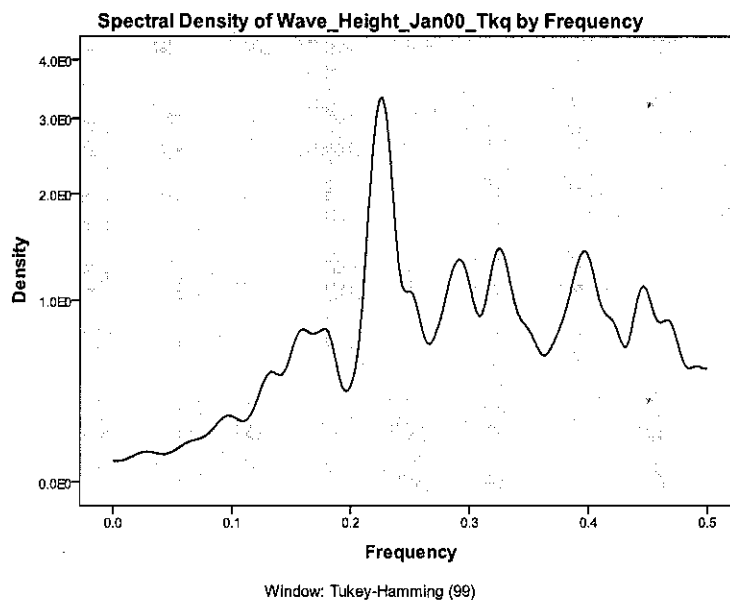
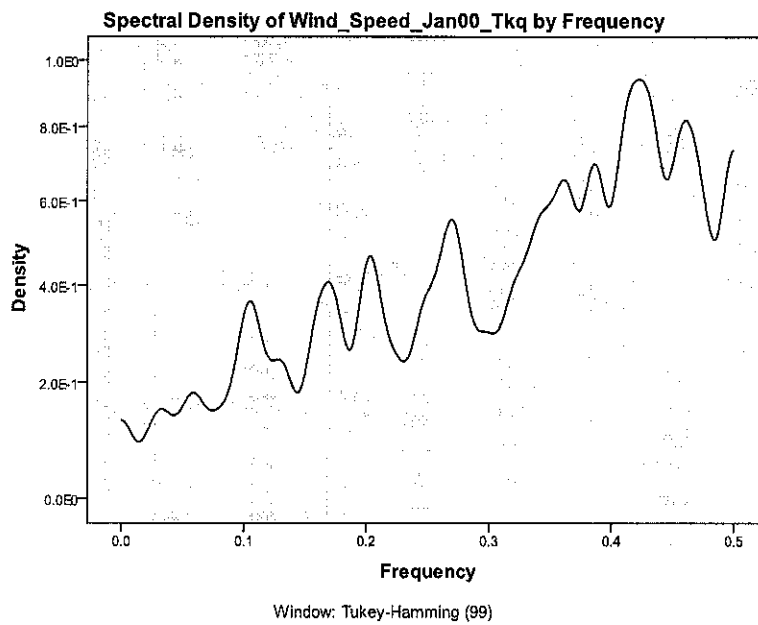
$$G_{xy} = \Delta_{xy}(f) + i \psi_{xy}(f)$$

Coherence Function:

$$\gamma^2(f) = \frac{|G_{xy}(f)|^2}{G_{xx}(f)G_{yy}(f)}$$

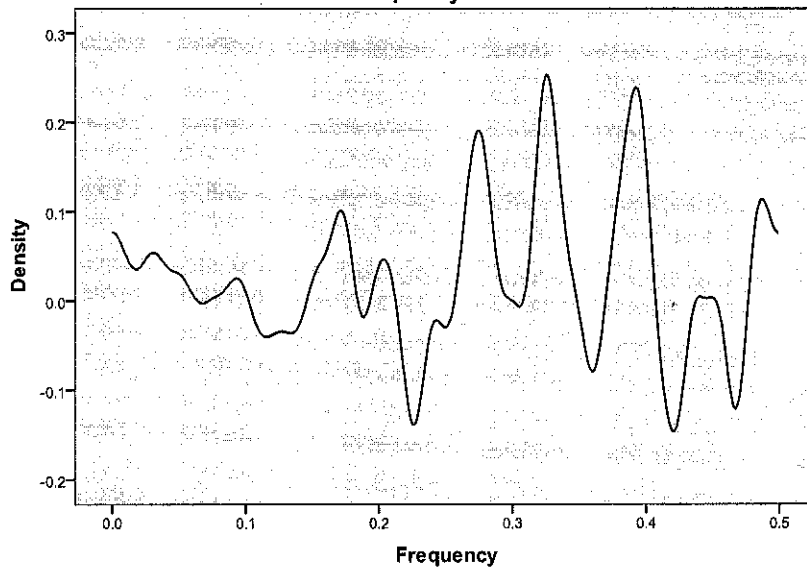
Frequency, Hz	Wind Spectrum, G_{xx}	Waves Spectrum, G_{yy}	Cospectral, Δ_{xy}	Quadrature Spectrum, ψ_{xy}	Cross Spectrum, G_{xy}	Coherence, γ_{xy}
0.05	0.1158	0.0629	0.0219	-0.021	0.00103	0.000146
0.1	0.2102	0.1545	0.0162	-0.035	-0.01885	0.010947
0.15	0.4022	0.2483	-0.002	-0.012	-0.0138	0.001908
0.2	0.2391	0.3827	-0.036	0.0336	-0.00199	4.32E-05
0.25	0.3729	0.6766	0.0276	-0.038	-0.01026	0.000417
0.3	0.3937	1.0753	0.0149	-0.126	-0.11079	0.028993
0.35	0.4348	0.6516	0.0248	-0.001	0.023643	0.001973
0.4	0.5015	1.0366	0.0751	-0.041	0.033659	0.002179
0.45	0.7443	0.5223	0.0405	0.0021	0.042593	0.004667
0.5	0.435	0.7218	0.1065	0	0.106472	0.036109

Tukau 2000 – Monsoon Season



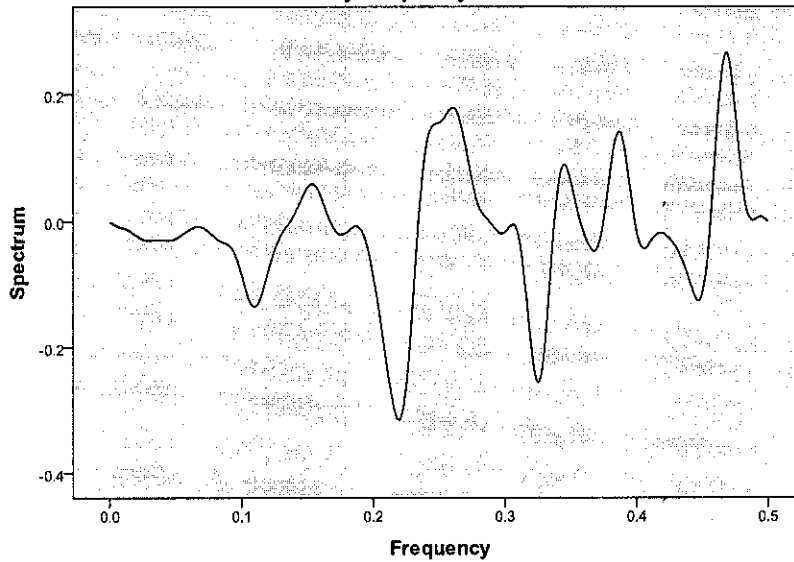
Frequency, Hz	Wind Spectrum, G_{xx}	Waves Spectrum, G_{yy}
0.05	0.1554	0.1239
0.1	0.335	0.2856
0.15	0.2194	0.6437
0.2	0.4506	0.4476
0.25	0.3875	1.0655
0.3	0.2989	1.1078
0.35	0.5987	0.7729
0.4	0.6007	1.3479
0.45	0.7082	1.0329
0.5	0.7355	0.54

Cospectral Density of Wind_Speed_Jan00_Tkq and Wave_Height_Jan00_Tkq by Frequency



Window: Tukey-Hamming (99)

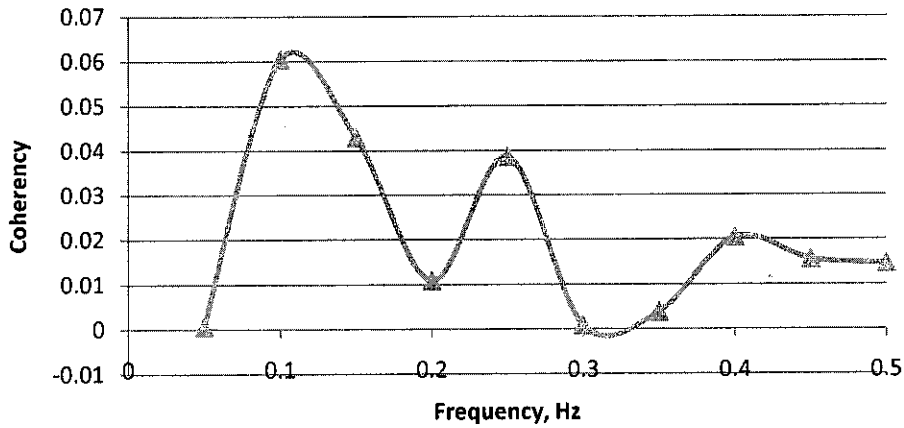
Quadrature Spectrum of Wind_Speed_Jan00_Tkq and Wave_Height_Jan00_Tkq by Frequency



Window: Tukey-Hamming (99)

Frequency, Hz	Cospectral, Δ_{xy}	Quadrature Spectrum, ψ_{xy}
0.05	0.0305	-0.027
0.1	0.0094	-0.085
0.15	0.0236	0.0543
0.2	0.0404	-0.087
0.25	-0.0298	0.156
0.3	-0.0005	-0.016
0.35	-0.0183	0.0604
0.4	0.1491	-0.02
0.45	0.0032	-0.11
0.5	0.0761	0

Coherence Function of Wind and Waves for Tukau 2000 - Monsoon Season



Cross Spectrum:

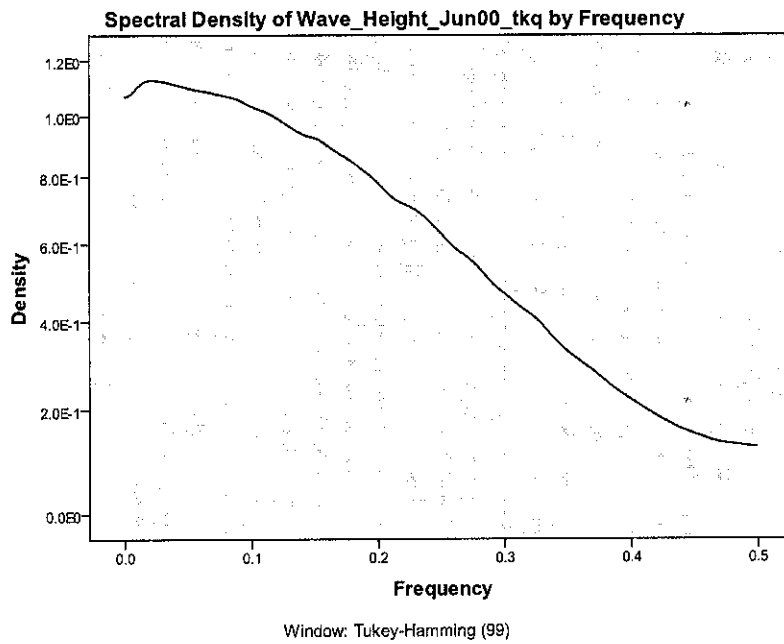
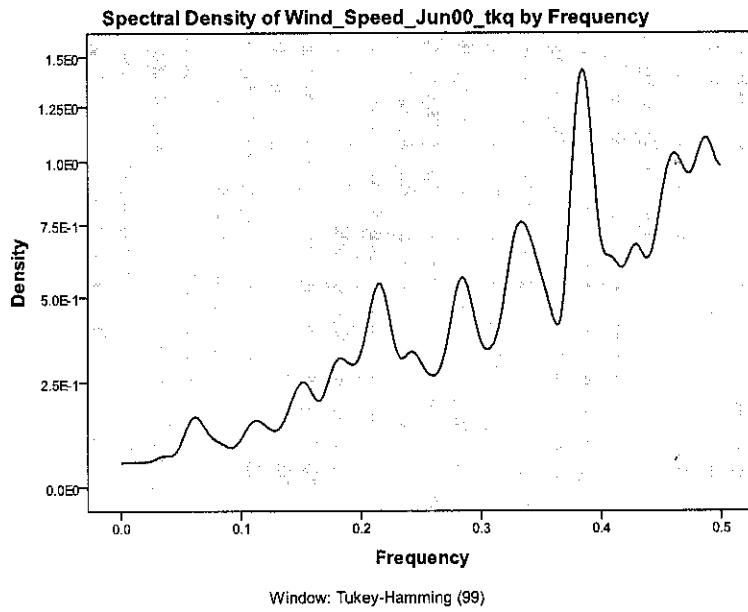
$$G_{xy} = \Delta_{xy}(f) + i \psi_{xy}(f)$$

Coherence Function:

$$\gamma^2(f) = \frac{|G_{xy}(f)|^2}{G_{xx}(f)G_{yy}(f)}$$

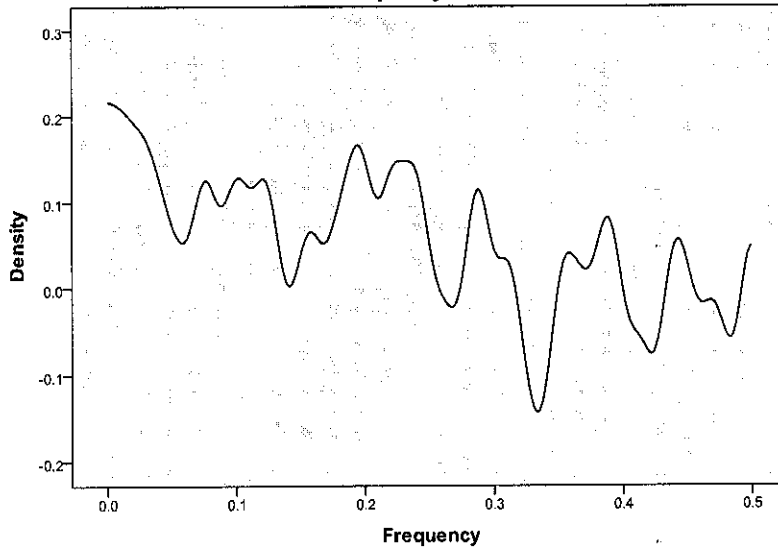
Frequency, Hz	Wind Spectrum, G_{xx}	Waves Spectrum, G_{yy}	Cospectral, Δ_{xy}	Quadrature Spectrum, ψ_{xy}	Cross Spectrum, G_{xy}	Coherence, γ_{xy}
0.05	0.1554	0.1239	0.0305	-0.027	0.003605	0.000675
0.1	0.335	0.2856	0.0094	-0.085	-0.07601	0.060392
0.15	0.2194	0.6437	0.0236	0.0543	0.077884	0.042955
0.2	0.4506	0.4476	0.0404	-0.087	-0.04683	0.010874
0.25	0.3875	1.0655	-0.0298	0.156	0.126197	0.03857
0.3	0.2989	1.1078	-0.0005	-0.016	-0.01684	0.000856
0.35	0.5987	0.7729	-0.0183	0.0604	0.042166	0.003843
0.4	0.6007	1.3479	0.1491	-0.02	0.128737	0.020466
0.45	0.7082	1.0329	0.0032	-0.11	-0.1067	0.015565
0.5	0.7355	0.54	0.0761	0	0.076136	0.014594

Tukau 2000 – Non Monsoon Season



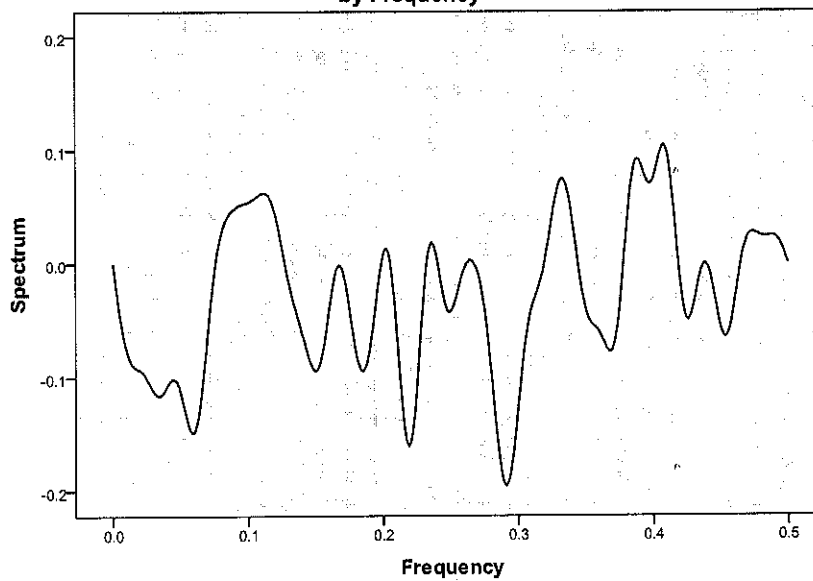
Frequency, Hz	Wind Spectrum, G_{xx}	Waves Spectrum, G_{yy}
0.05	0.101	1.0997
0.1	0.1102	1.0335
0.15	0.2499	0.9247
0.2	0.3346	0.7802
0.25	0.3018	0.6285
0.3	0.361	0.4689
0.35	0.5718	0.3277
0.4	0.6848	0.221
0.45	0.8541	0.15
0.5	0.9807	0.125

Cospectral Density of Wind_Speed_Jun00_tkq and Wave_Height_Jun00_tkq by Frequency



Window: Tukey-Hamming (99)

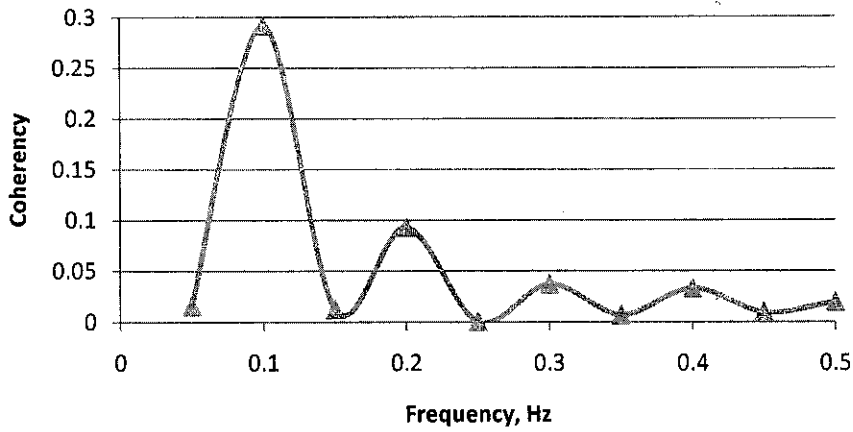
Quadrature Spectrum of Wind_Speed_Jun00_tkq and Wave_Height_Jun00_tkq by Frequency



Window: Tukey-Hamming (99)

Frequency, Hz	Cospectral, Δ_{xy}	Quadrature Spectrum, ψ_{xy}
0.05	0.0727	-0.114
0.1	0.1277	0.0544
0.15	0.0409	-0.094
0.2	0.1469	0.0086
0.25	0.0481	-0.042
0.3	0.0439	-0.123
0.35	0.0066	-0.042
0.4	-0.006	0.0767
0.45	0.025	-0.059
0.5	0.0489	0

Coherence Function of Wind and Waves for Tukau 2000 - Non Monsoon



Cross Spectrum:

$$G_{xy} = \Delta_{xy}(f) + i \psi_{xy}(f)$$

Coherence Function:

$$\gamma^2(f) = \frac{|G_{xy}(f)|^2}{G_{xx}(f)G_{yy}(f)}$$

Frequency, Hz	Wind Spectrum, G_{xx}	Waves Spectrum, G_{yy}	Cospectral, Δ_{xy}	Quadrature Spectrum, ψ_{xy}	Cross Spectrum, G_{xy}	Coherence, γ_{xy}
0.05	0.101	1.0997	0.0727	-0.114	-0.04172	0.015678
0.1	0.1102	1.0335	0.1277	0.0544	0.182114	0.291289
0.15	0.2499	0.9247	0.0409	-0.094	-0.05341	0.012347
0.2	0.3346	0.7802	0.1469	0.0086	0.155513	0.092635
0.25	0.3018	0.6285	0.0481	-0.042	0.006237	0.000205
0.3	0.361	0.4689	0.0439	-0.123	-0.07899	0.036863
0.35	0.5718	0.3277	0.0066	-0.042	-0.03593	0.006889
0.4	0.6848	0.221	-0.006	0.0767	0.070625	0.032963
0.45	0.8541	0.15	0.025	-0.059	-0.03435	0.009212
0.5	0.9807	0.125	0.0489	0	0.048859	0.019469